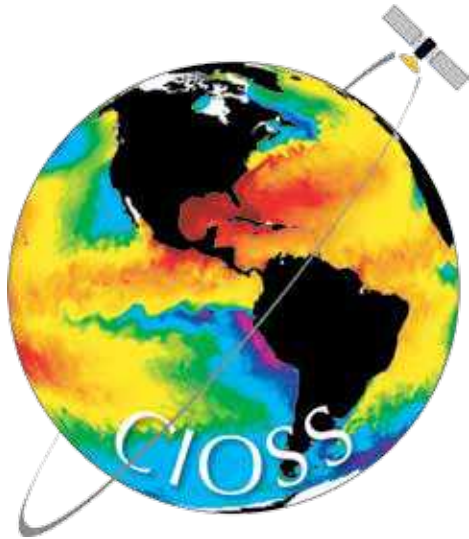


The Influence of Nonlinear Mesoscale Eddies on Oceanic Chlorophyll



Peter Gaube
Dudley Chelton
Pete Strutton

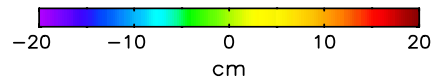
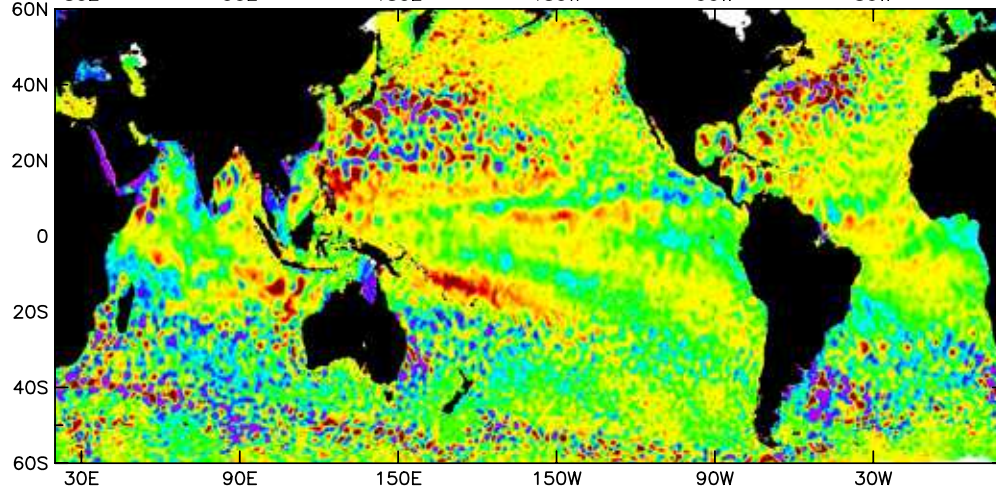
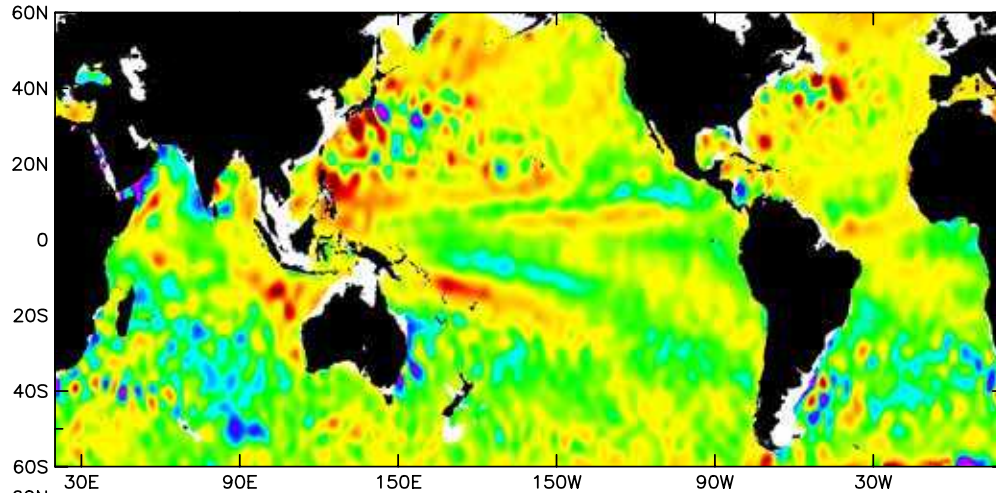


Overview

1. Tracking eddies in merged altimetry data
2. Observations of ecosystems trapped within nonlinear eddies
3. Westward co-propagation of SSH and CHL

Observations of Nonlinear Mesoscale Eddies

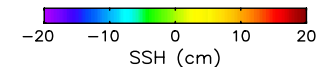
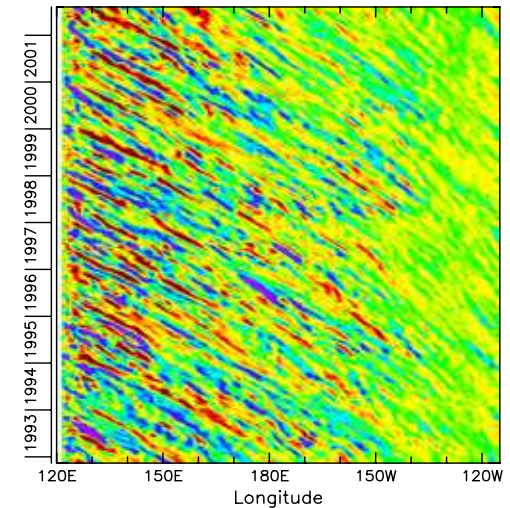
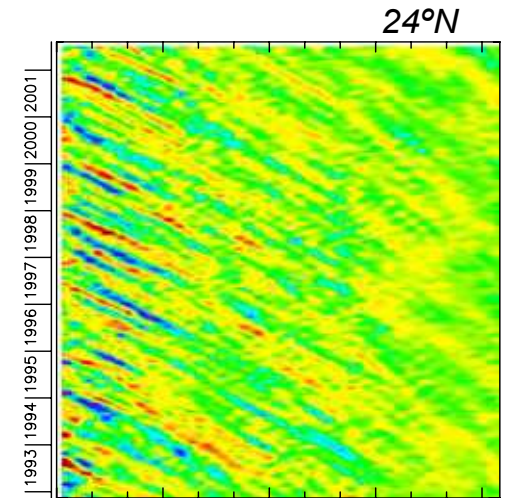
SSH From TOPEX Only
and from the Merged TOPEX and ERS-1/2 Data (Ducet et al. 2000)



There are 2495 eddies in this map

TOPEX
Only

TOPEX
+
ERS-1/2



Eddies of the California Current

eddies tracked in merged altimetry observations (Chelton *et al.*, 2011)

Automated Eddy Tracking

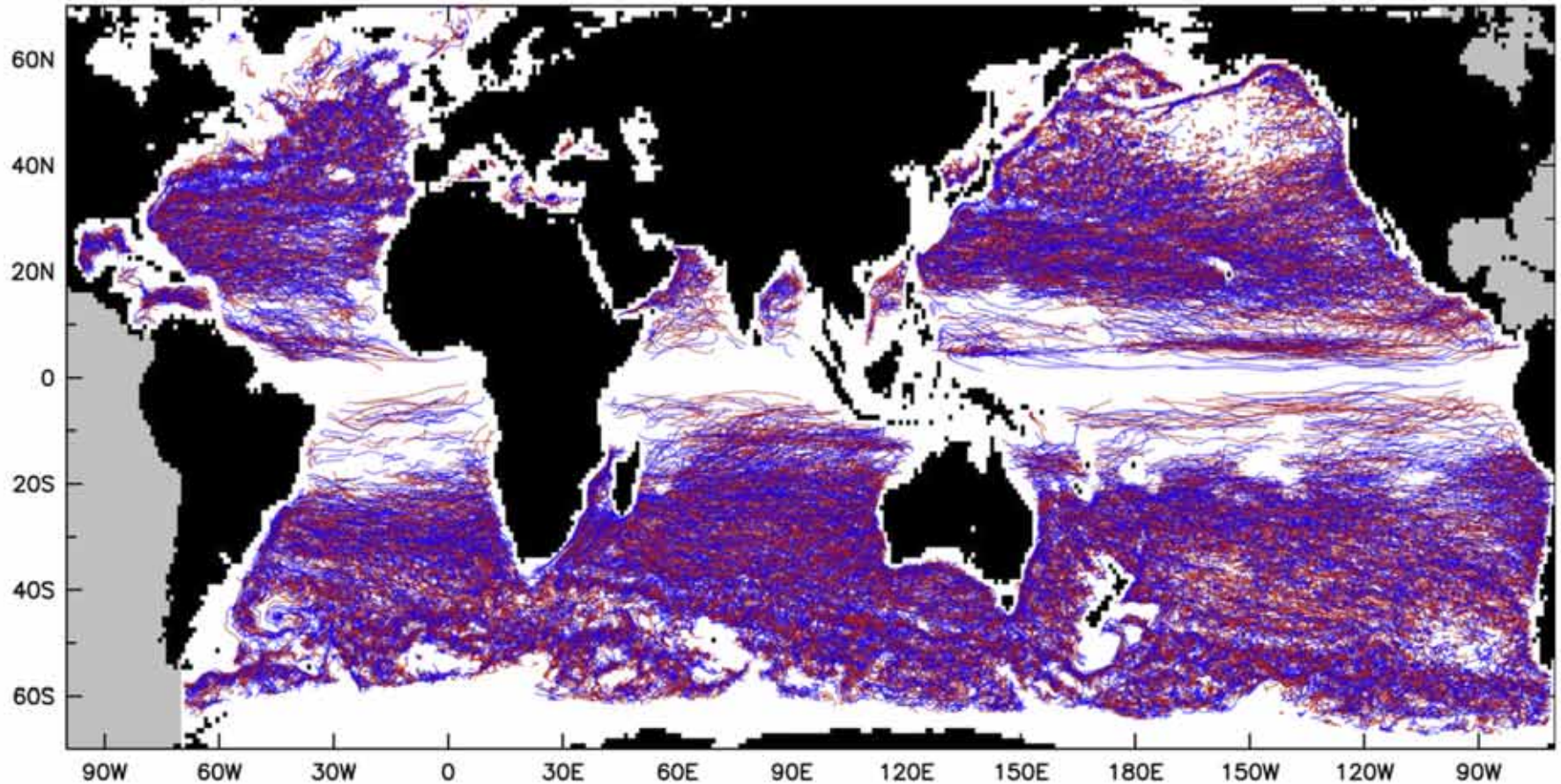
tracks of long-lived eddies

(a)

Lifetimes ≥ 16 weeks

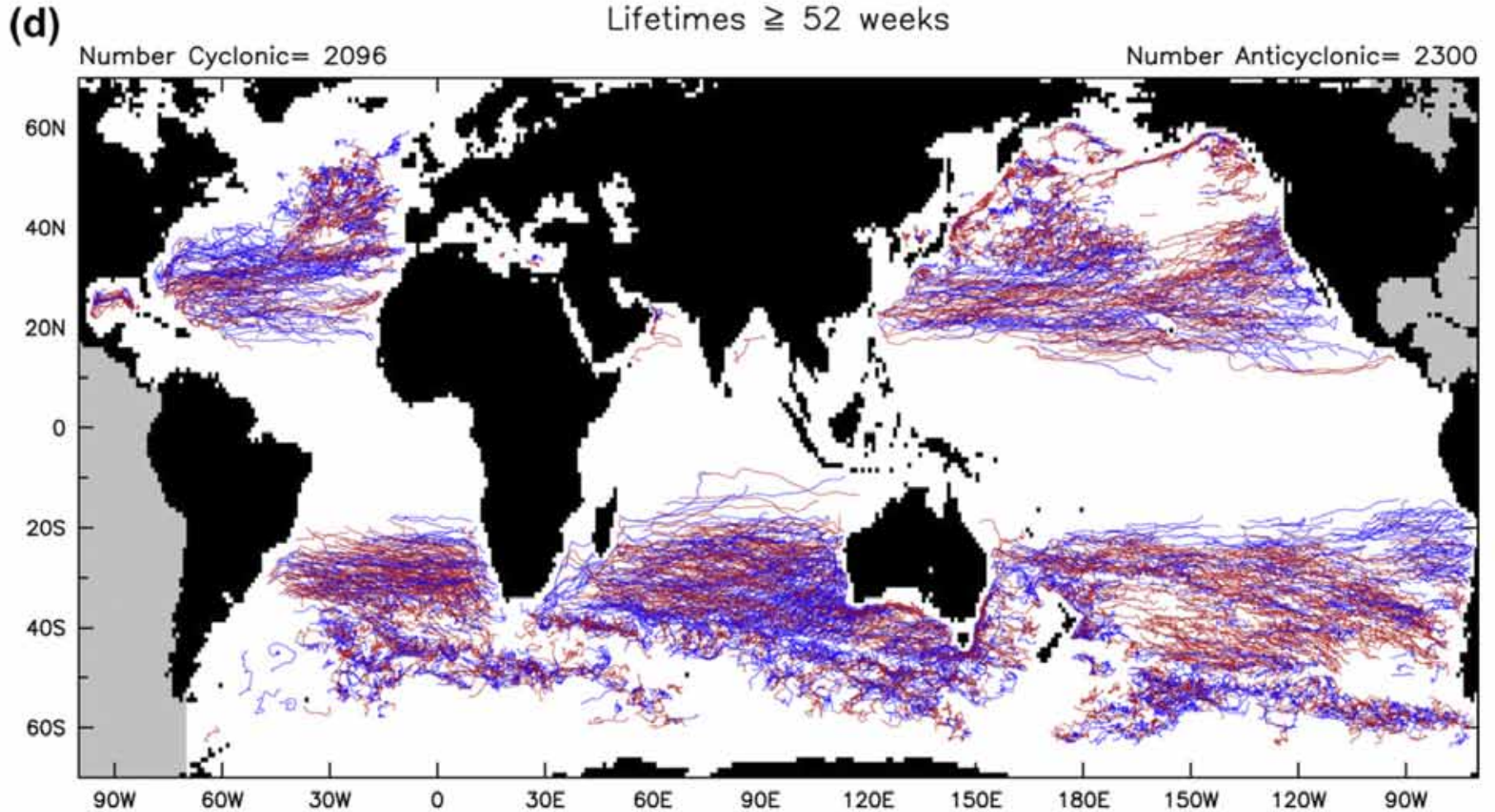
Number Cyclonic=18469

Number Anticyclonic=17422



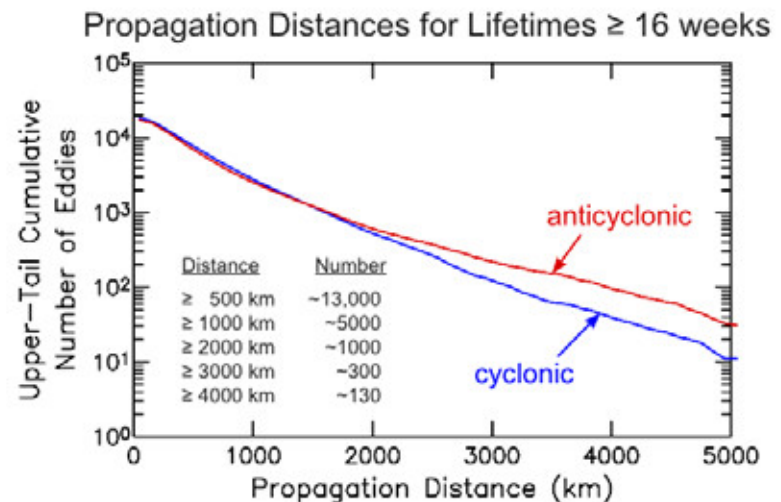
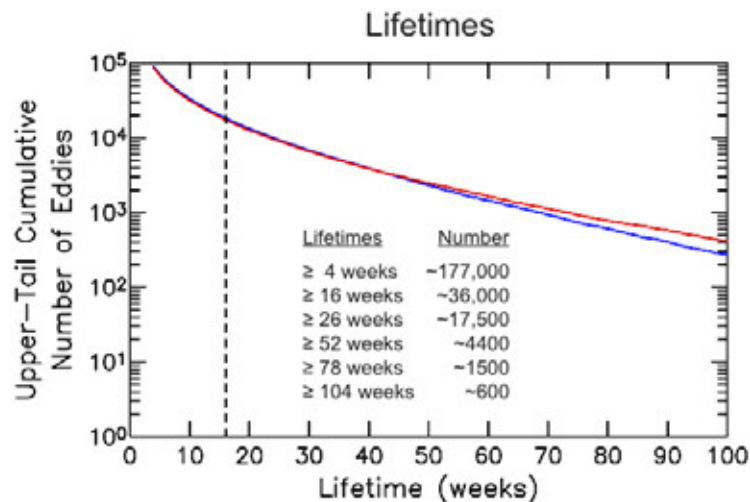
Automated Eddy Tracking

tracks of *really* long lived eddies



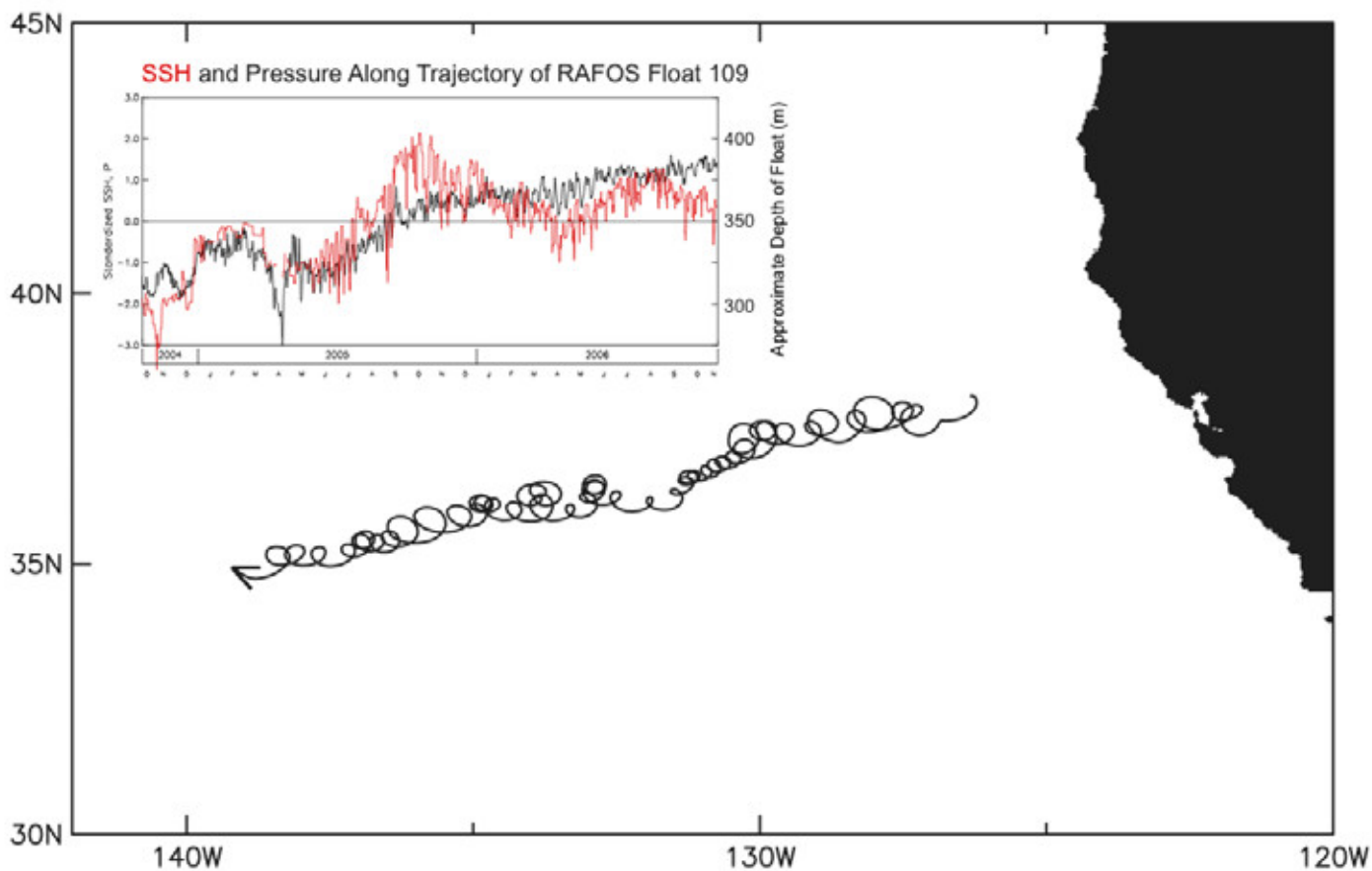
Results from Application of an Automated Eddy Identification and Tracking Procedure Applied to 16 Years of SSH Data

Distributions of Eddy Lifetimes and Propagation Distances



Trajectory of NPGS RAFOS Float 109 in the California Current

31 August 2005 - 8 November 2006
(Courtesy of Curt Collins, NPGS)



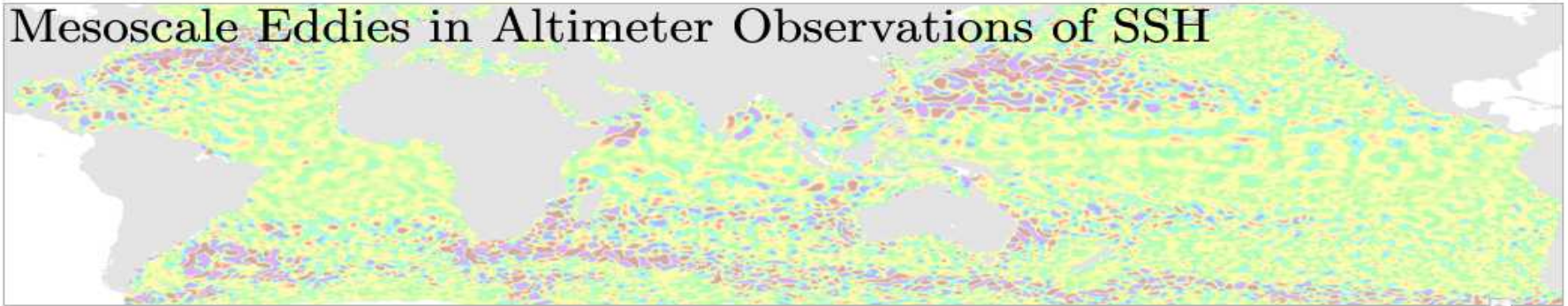
The depth range of the float was about 310-380 m.

Animation of NPGS RAFOS Float 109 in the California Current

31 August 2005 - 8 November 2006

(Courtesy of Curt Collins, NPGS)

Mesoscale Eddies in Altimeter Observations of SSH



[Home Page](#)

[NetCDF Data File](#)

[ASCII Data File](#)

[Geographical Domain &
Sample Output](#)

[Contact](#)

[COAS](#)

[AVISO](#)

[OSU Disclaimer](#)

Mesoscale Eddies in Altimeter Observations of SSH

Dudley B. Chelton and Michael G. Schlax

The trajectories at 7-day time steps of approximately 177,000 mesoscale eddies in the SSH fields in the [AVISO Reference Series](#) are available for public access for the 16-year period October 1992 through December 2008. The details of this eddy dataset and the characteristics of the eddies (their amplitudes, radius scales and rotational speeds) are described in [Chelton et al. \(2011\)](#). The eddies retained in this dataset are restricted to lifetimes of 4 weeks or longer.

The main text of this paper summarizes a detailed analysis of the eddies with lifetimes of 16 weeks and longer.

Appendices A.1 - A.3 assess the filtering properties of the objective analysis procedure used by AVISO to construct the SSH fields from which the eddies were identified and tracked.

Appendices B.1 - B.5 describe the details of the eddy identification and tracking procedure and Appendix C assesses the adequacy of the procedure.

Reference

Chelton, D. B., M. G. Schlax, and R. M. Samelson, 2011: [Global observations of nonlinear mesoscale eddies](#). *Prog. Oceanogr.*, **91**, 167-216.

Disclaimer: These data are provided "as is". In no event shall the providers be liable for any damages, including without limitation, damages resulting from lost profits or revenue, or any special, incidental, or consequential damages, arising out of the use of these data. While every effort has been made to ensure that these data are accurate and reliable, the accuracy and reliability of these data is not guaranteed or warranted in any way and the providers disclaim liability of any kind whatsoever, including, without limitation, liability for quality, performance, merchantability and fitness for a particular purpose arising out of the use, or inability to use these data.

Copyright © 2011. Last Updated: 22 February 2011.

<http://cioss.coas.oregonstate.edu/eddies/>

Who is using the eddies database?



Summary: Automated Eddy Tracking

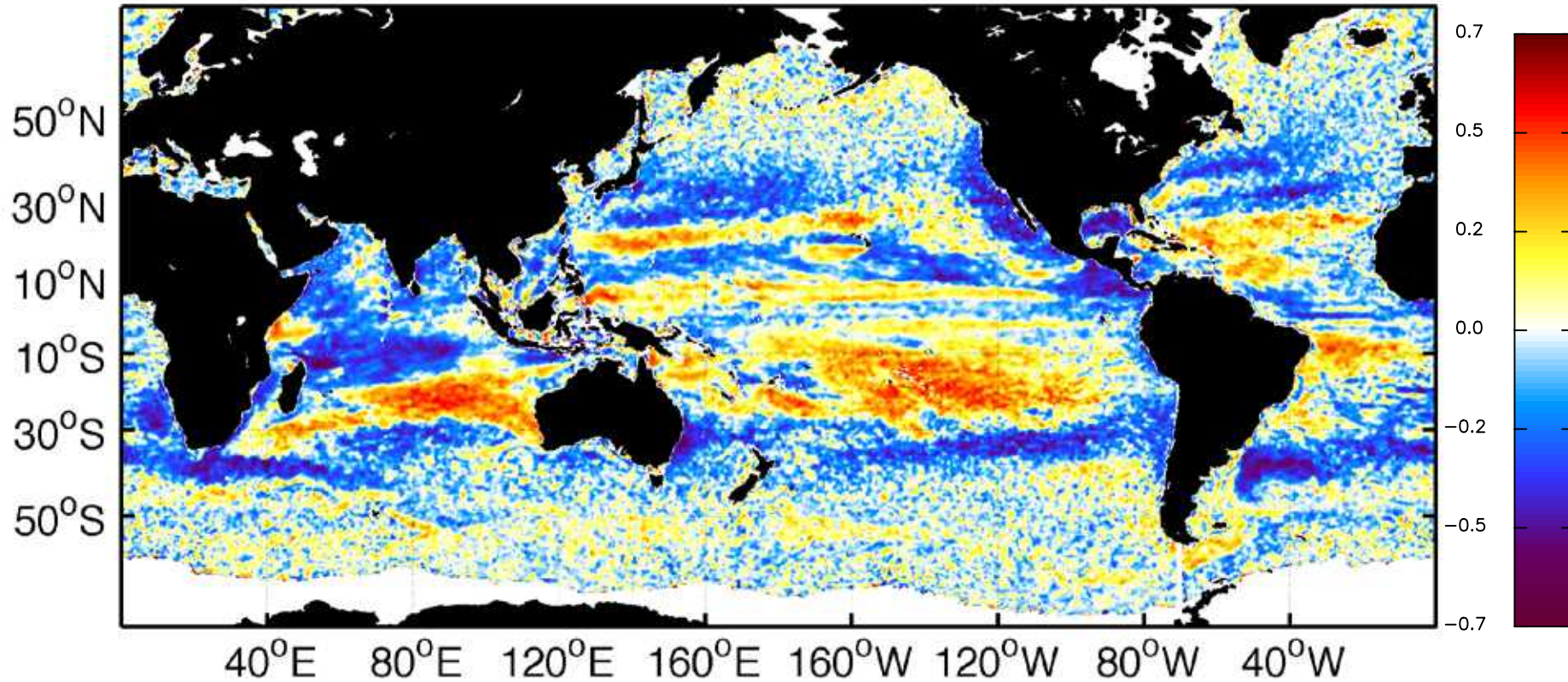
Chelton et al., 2011 Progress in Oceanography

- Eddies are identified as close geostrophic streamlines in high-pass filtered merged SSH fields
- Eddies with radial scales of ~ 200 to ~ 50 km can be tracked in SSH fields constructed by merging altimeters in different orbits.
- Over 150,000 eddies with lifetimes greater than 4 weeks have been tracked over the last 16 years.
- The methodologies used to track eddies can be applied to a variety of fields including SSH derived from eddy resolving ocean models to wide-swath altimetry measurements (SWOT).

Where do eddies influence marine ecosystems?

the influence of eddies on marine ecosystems is regionally dependent

SSH-CHL Cross Correlation

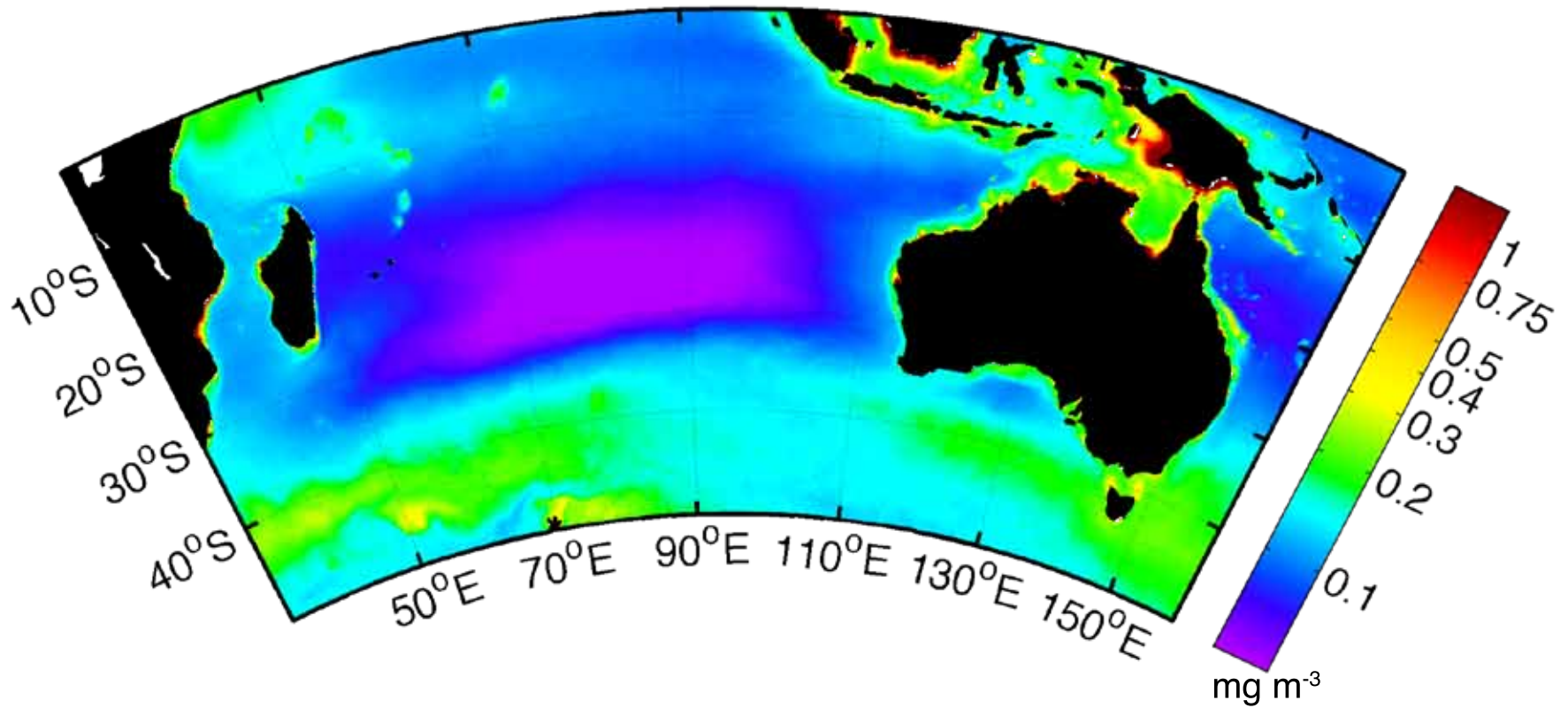


Regions of positive correlation are associated with CHL blooms in anticyclonic eddies

Regions of negative correlation are representative of cyclonic eddies driving CHL blooms

The Oligotrophic South Indian Ocean

average \log_{10} chlorophyll-a from SeaWiFS 2001-2008

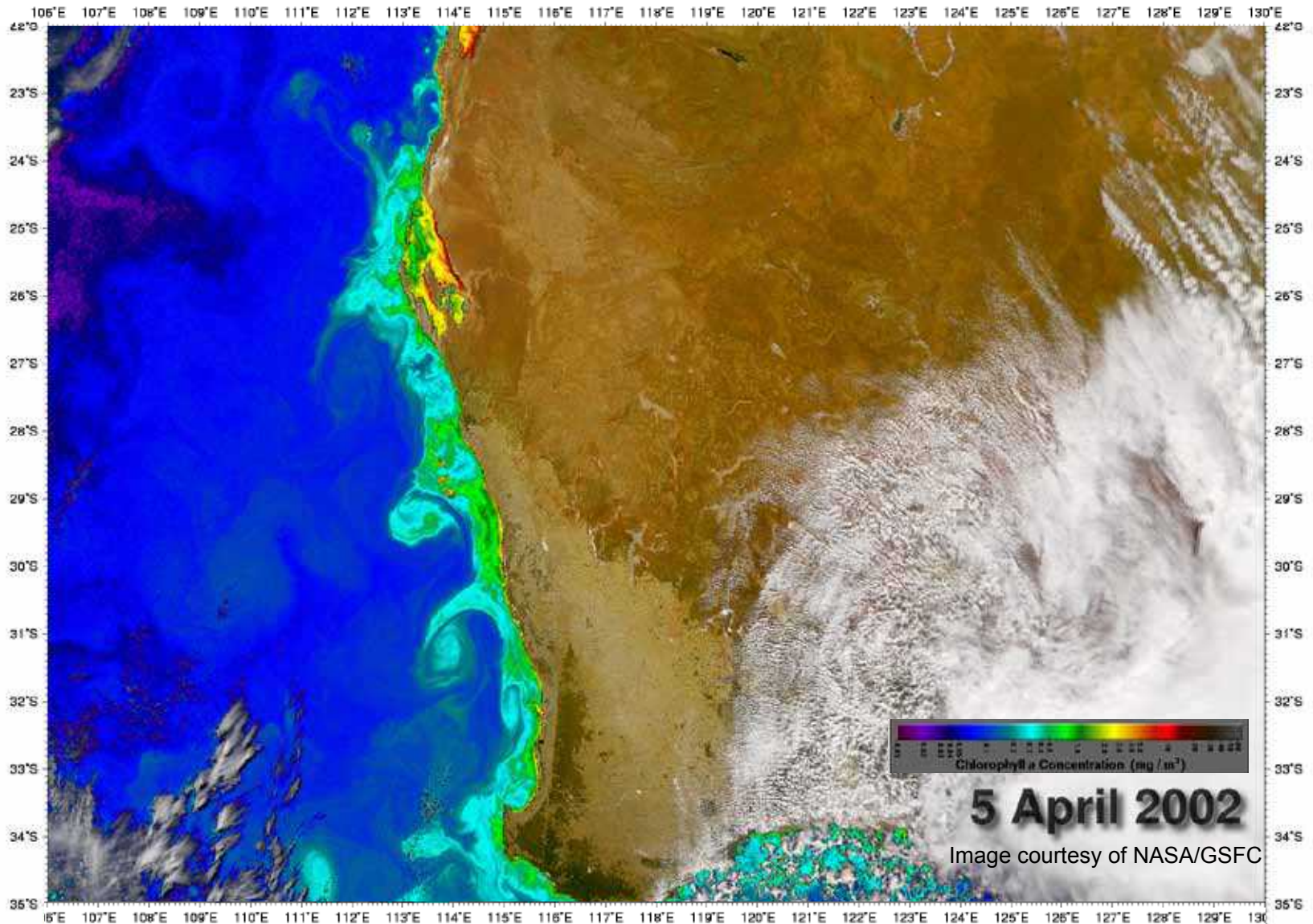


Eddies of the Indian Ocean

eddies tracked in merged altimetry observations (Chelton *et al.*, 2011)

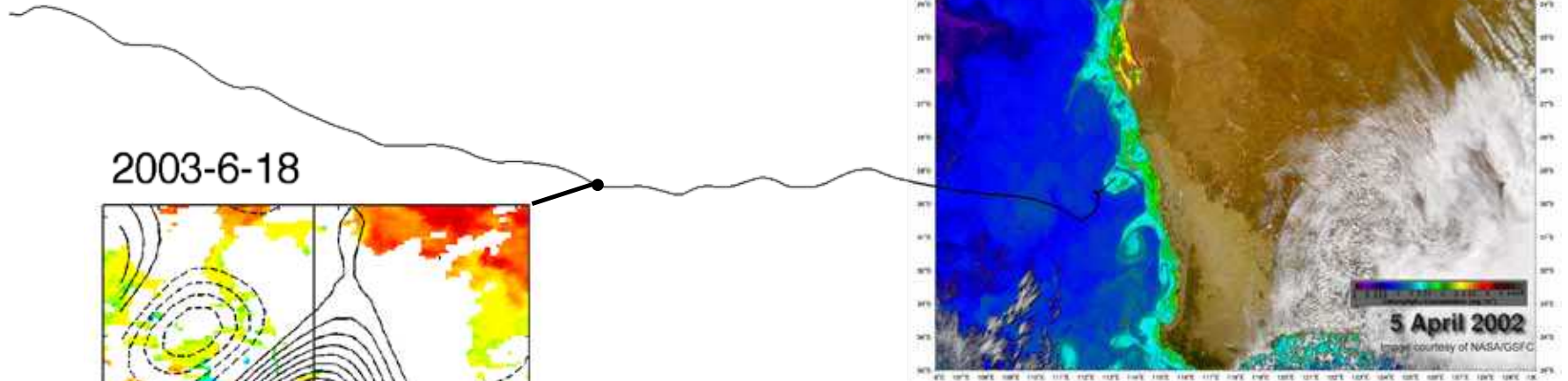
Observing Eddy-Induced Ecosystem Perturbations

SeaWiFS True Color with Chlorophyll-a Overlaid

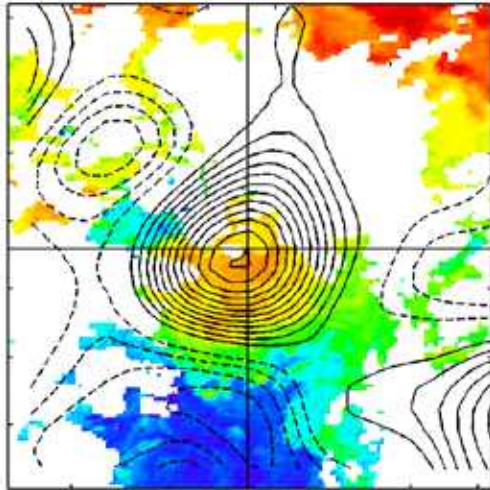


Case Study: A long-lived Leeuwin Current Anticyclone

this particular eddy was tracked for a total of 122 weeks



2003-6-18

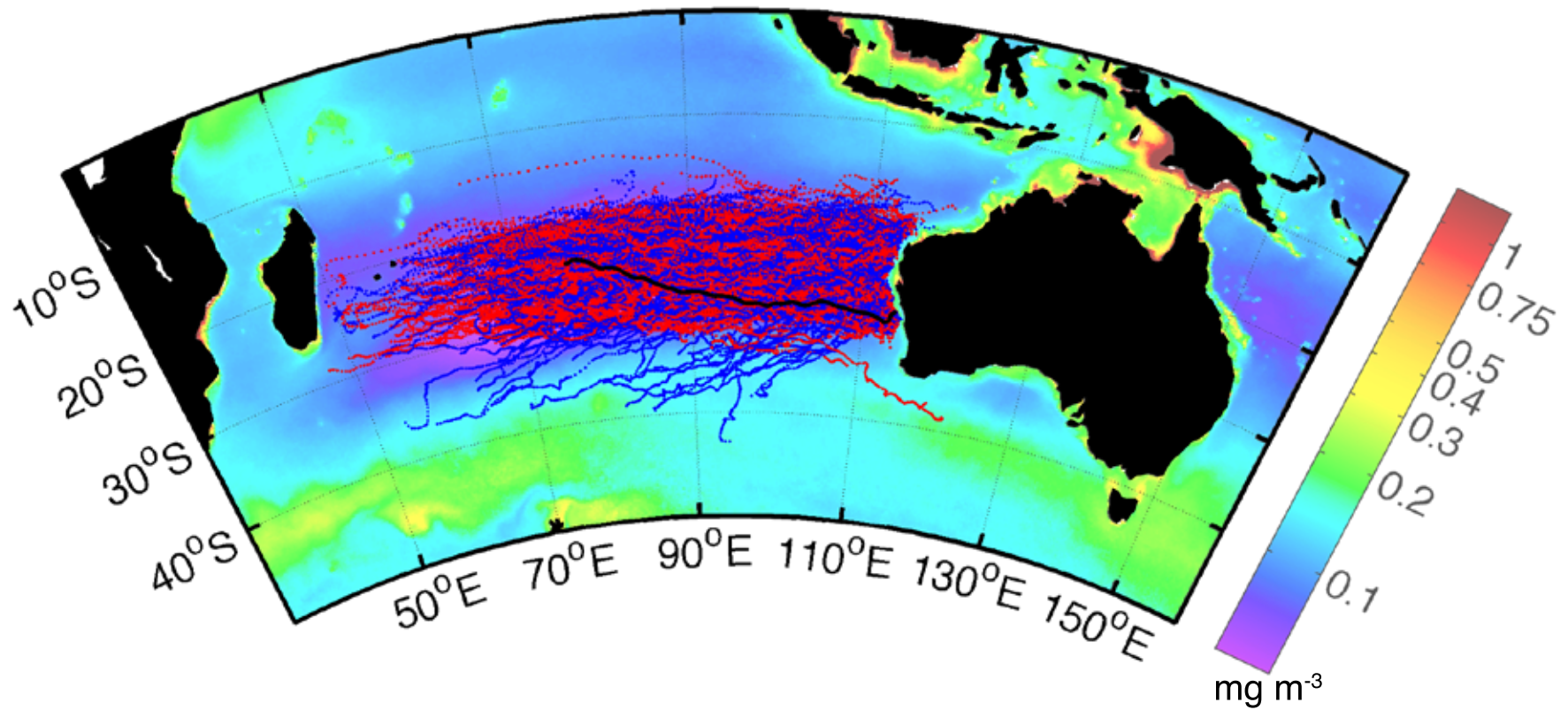


MODIS Aqua 1km
Chlorophyll-a

Even a full year after its formation, the core of this eddy still contains a trapped phytoplankton bloom.

Eddies Spawned from the Leeuwin Current

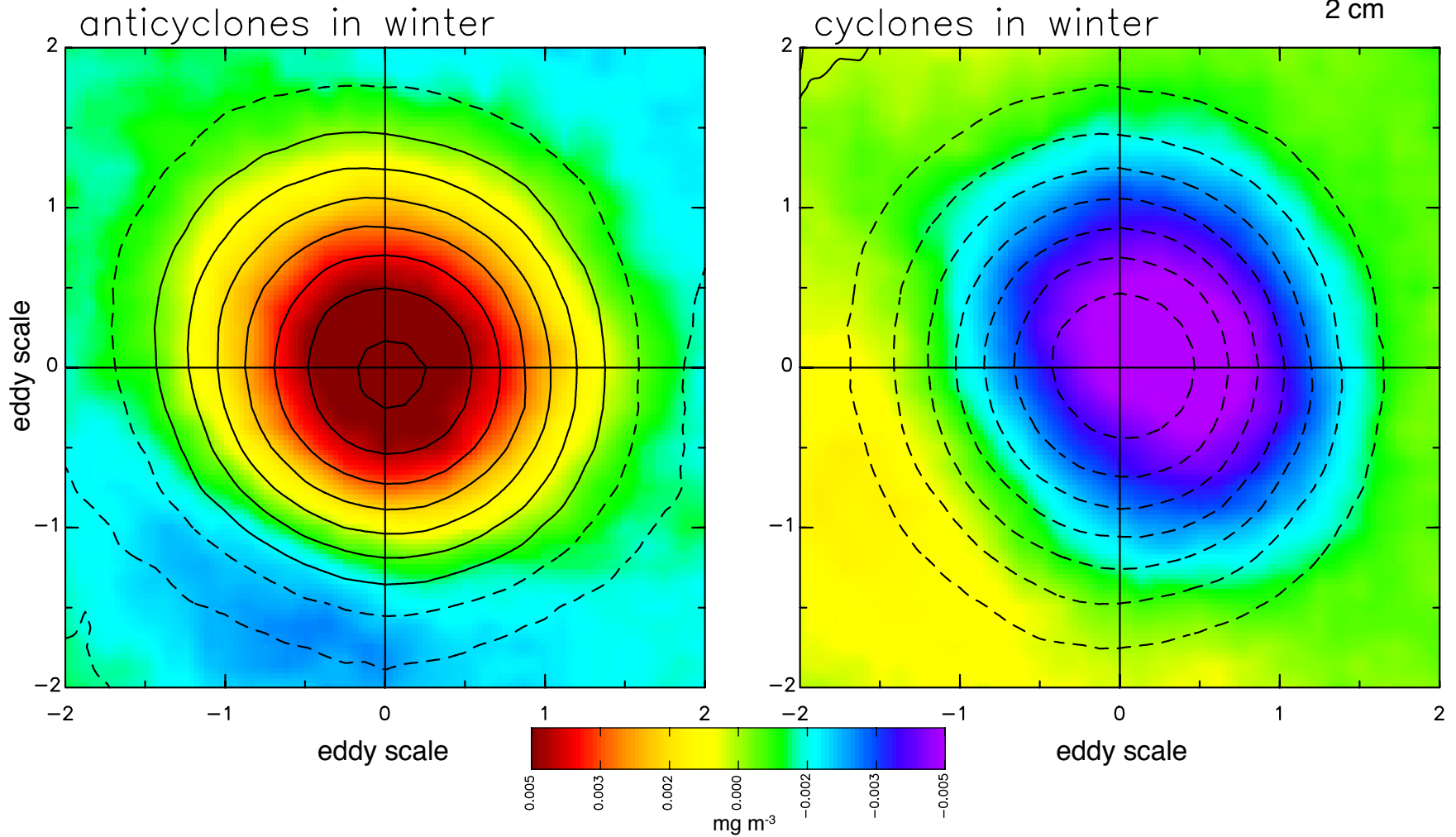
a total of 734 anticyclonic and 818 cyclonic long-lived eddies were tracked from 2000-2008



Composite Averaged Chlorophyll Anomalies

filtered SeaWiFS chlorophyll with contours of AVISO SSH

contour interval
2 cm



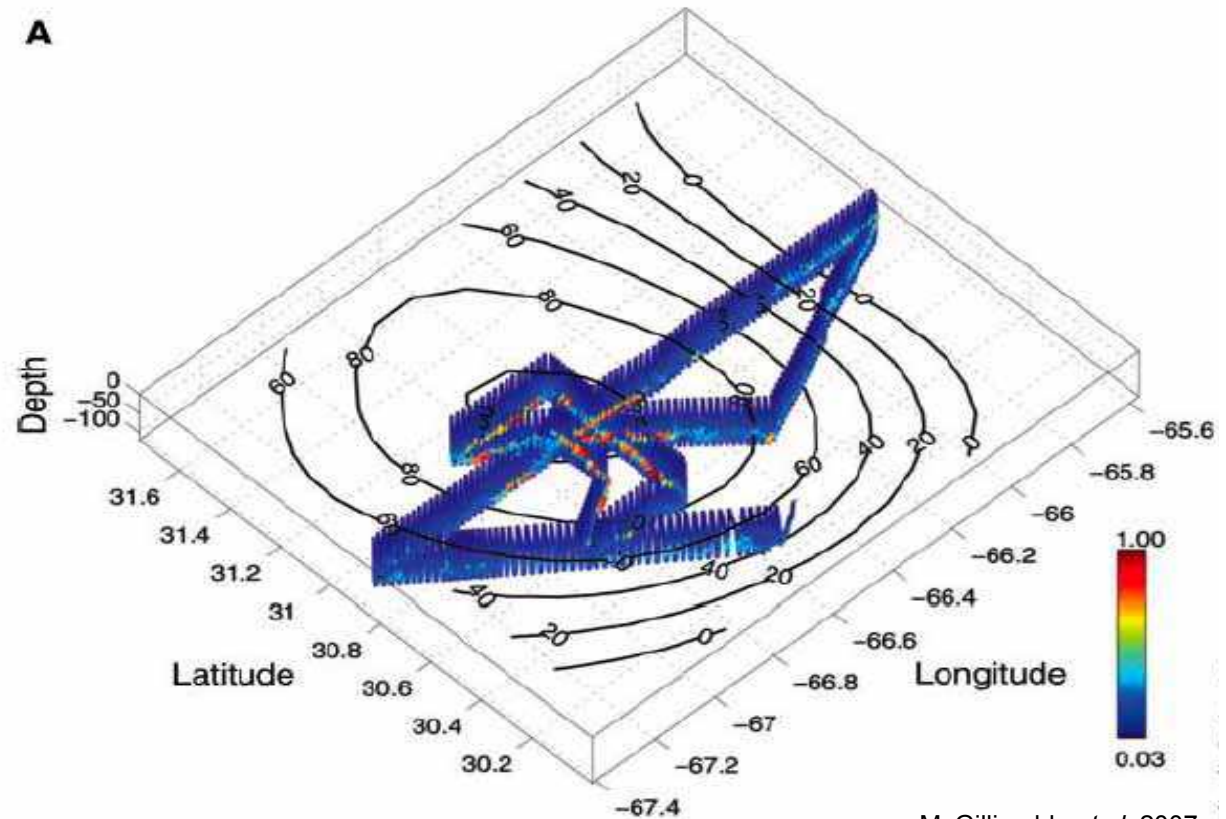
What drives upwelling in the cores of anticyclonic eddies?

Eddy-Induced Ekman Pumping

In 2007 a ship survey of an anticyclone in the Sargasso Sea revealed a large phytoplankton bloom at its core with primary production rates 4 x that of the previously observed local maximum.

Dye released in the core of the anticyclonic eddy was upwelled at a rate estimated to be $\sim 40 \text{ cm day}^{-1}$

Ekman pumping rates calculated from QuikSCAT compared well to the rates estimated from the dye release.

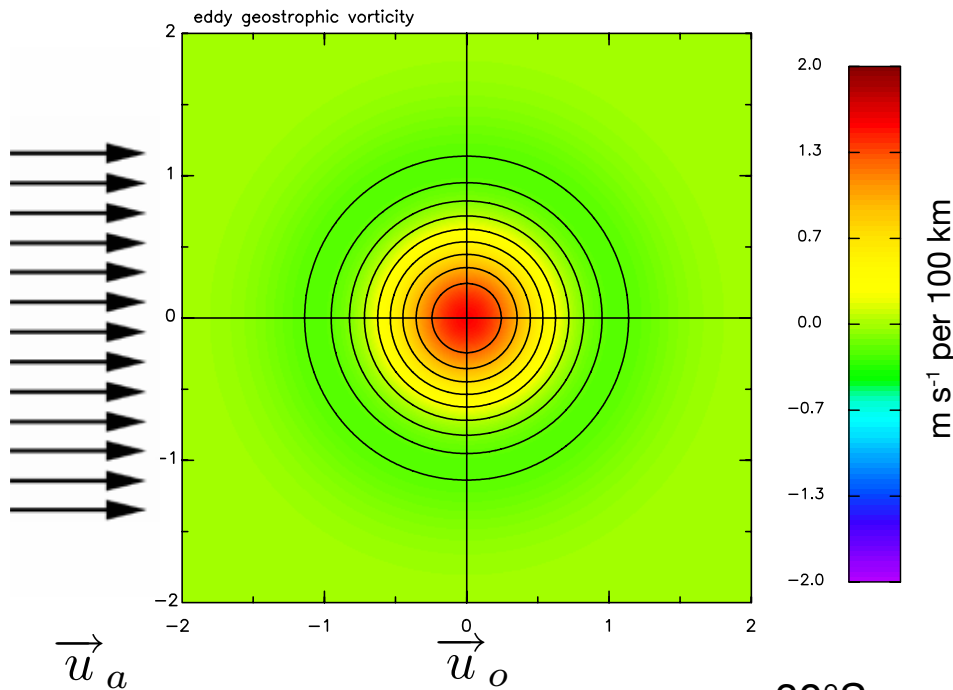


Eddy-Induced Ekman Pumping

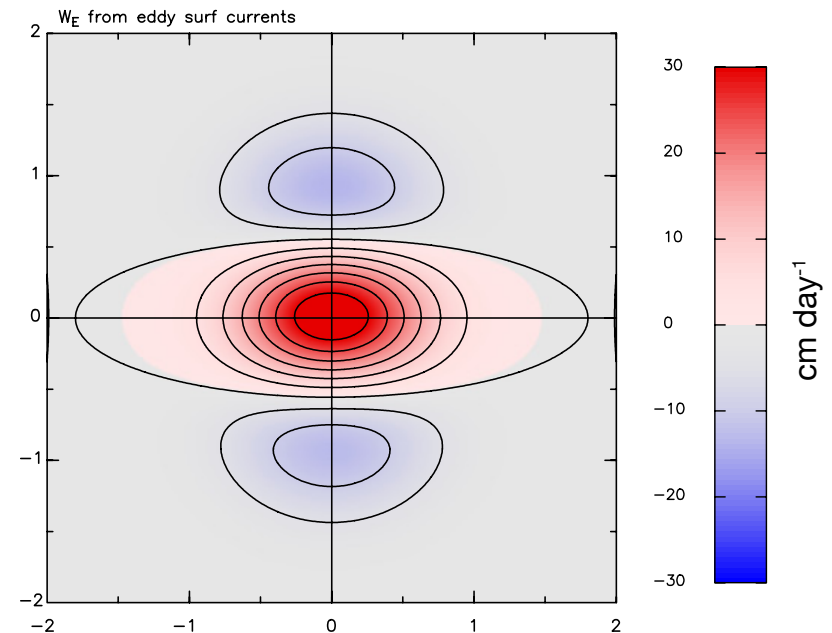
How it works:

- The surface circulation of an eddy can induce Ekman pumping in a uniform wind field.

Eddy Vorticity



Ekman Pumping



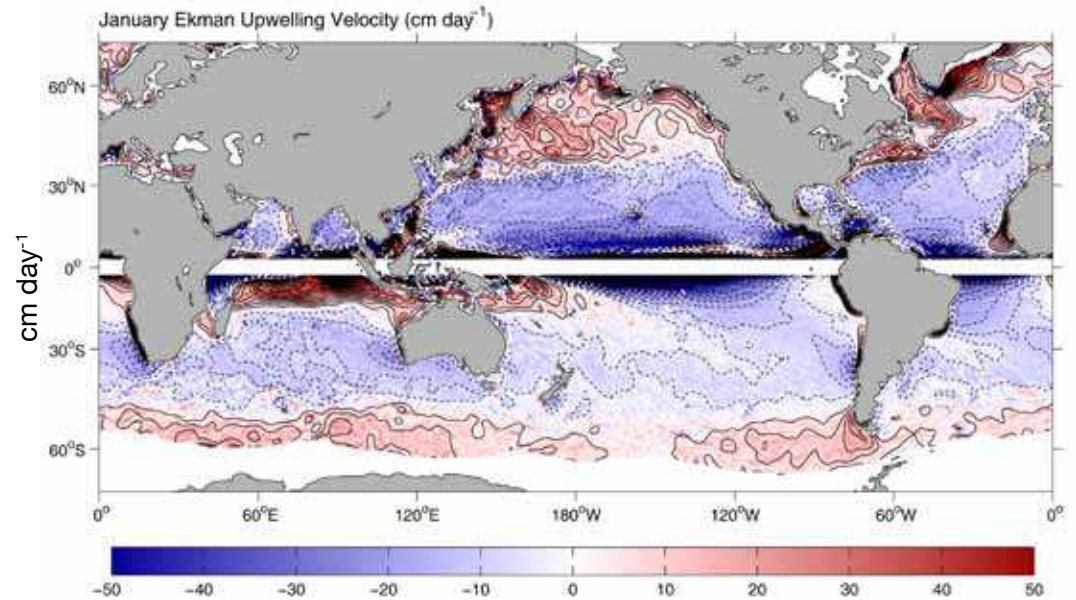
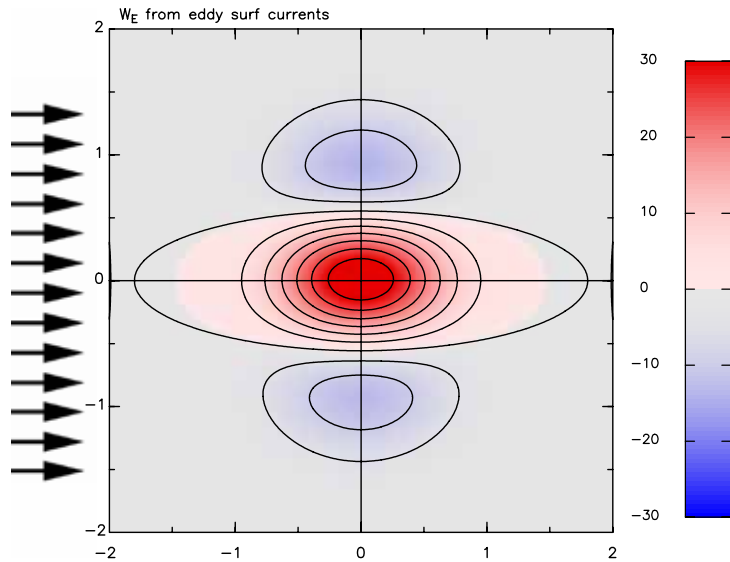
$$\vec{\tau} = \rho C_D |u_{rel}| \vec{u}_{rel}$$

$$\vec{u}_{rel} = \vec{u}_a - \vec{u}_o$$

- 30°S
- 20 cm amp.
- 10 ms⁻¹ wind
- Max current
40 cm s⁻¹

$$W_E = \frac{1}{\rho f} \nabla \times \vec{\tau}$$

Eddy-Induced Ekman Pumping



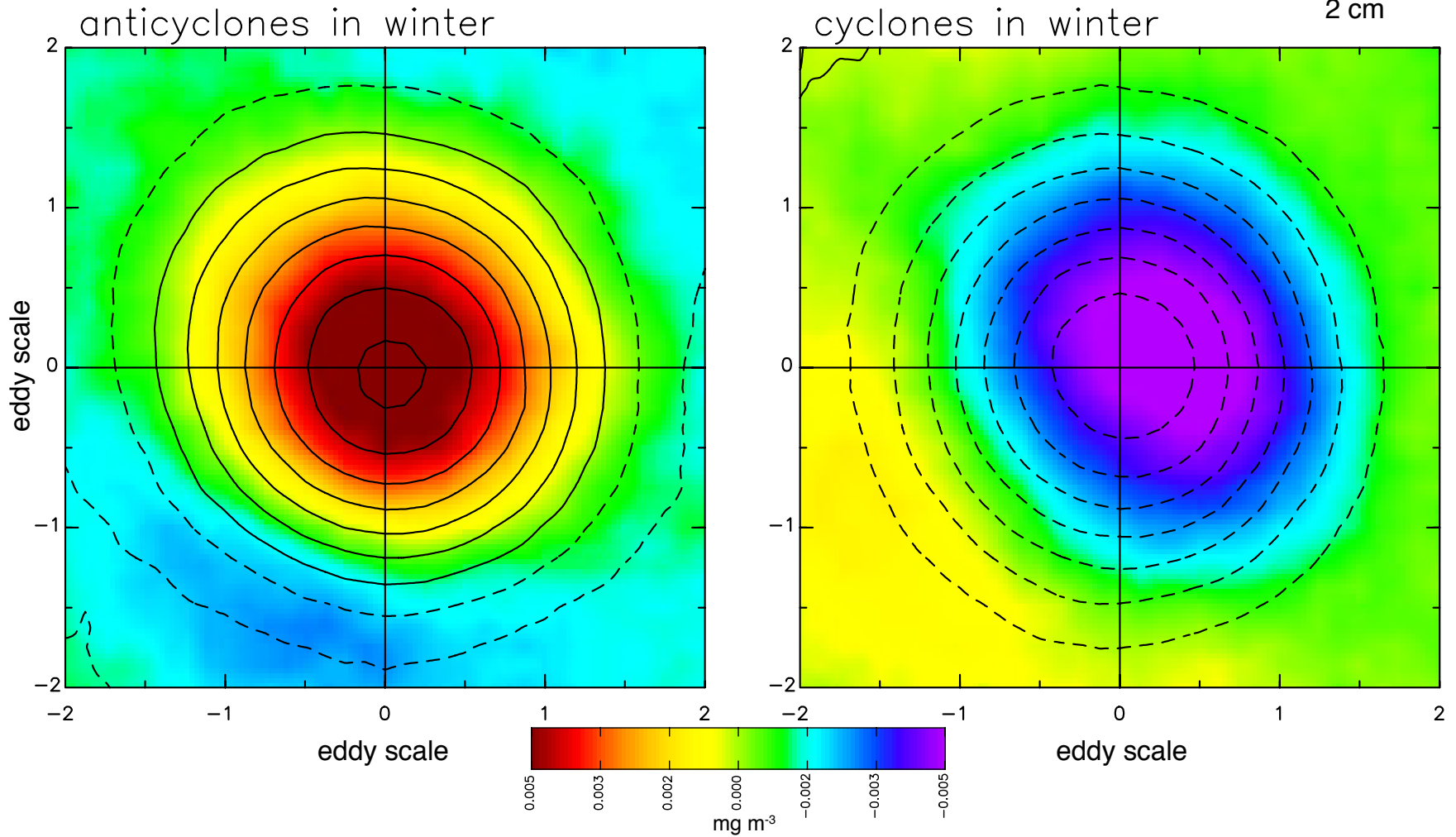
Risien and Chelton, 2008

- *Eddy-induced Ekman pumping is of the same order of magnitude as basin scale Ekman pumping*

Composite Averaged Chlorophyll Anomalies

filtered SeaWiFS chlorophyll with contours of AVISO SSH

contour interval
2 cm

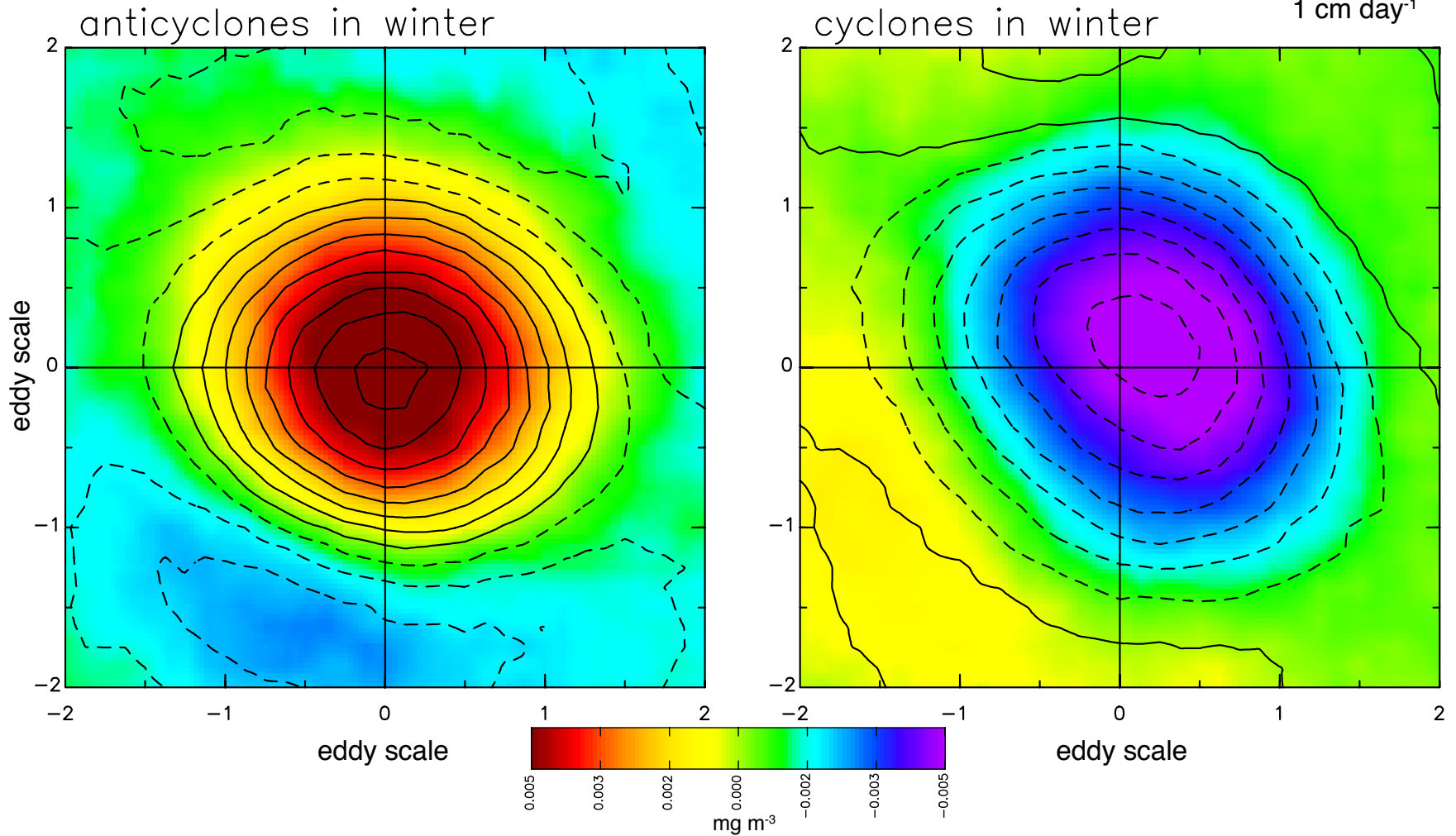


Can eddy-induced Ekman pumping account for the spatial structure of these CHL blooms?

Composite Averaged Chlorophyll Anomalies

filtered SeaWiFS chlorophyll with contours of QuikSCAT Ekman pumping

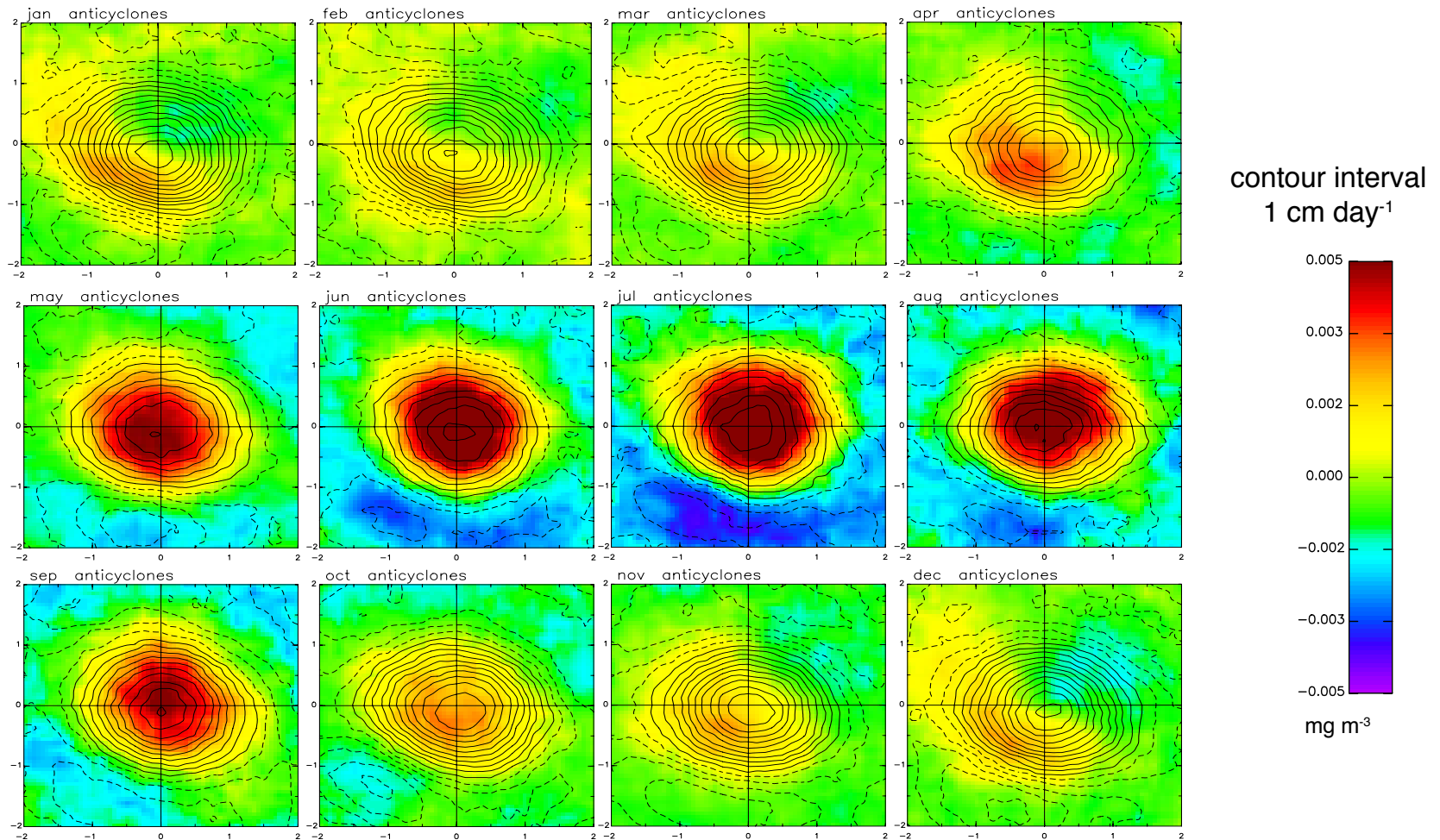
contour interval
1 cm day⁻¹



- Seasonally (May - September), we observed enhanced CHL at the cores of anticyclonic eddies.
- Negative CHL anomalies are a persistent feature of cyclonic eddies in this region.

Composite Averaged Chlorophyll Anomalies by Month

filtered SeaWiFS chlorophyll with contours of QuikSCAT Ekman pumping (anticyclones)

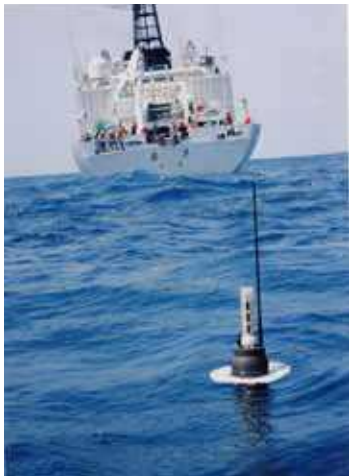
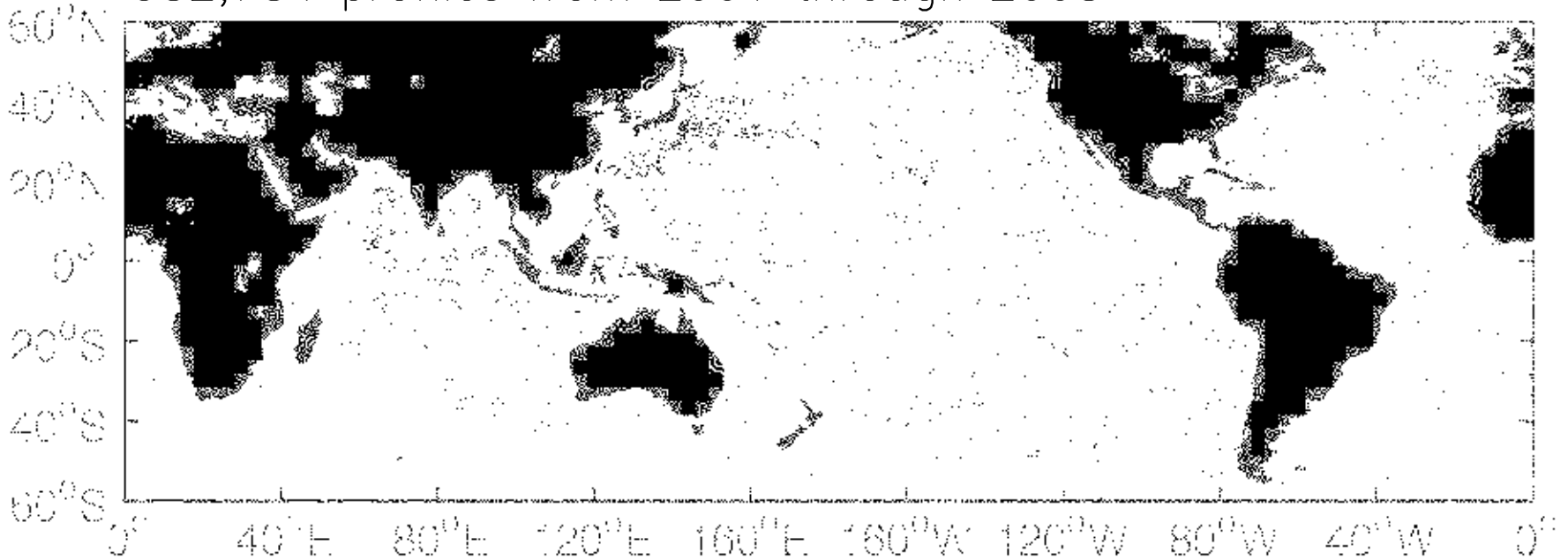


What is driving the seasonal response of CHL to eddy-induced Ekman pumping?

ARGO Floats

ARGO floats offer insight into the vertical structure of eddies

382,784 profiles from 2001 through 2008

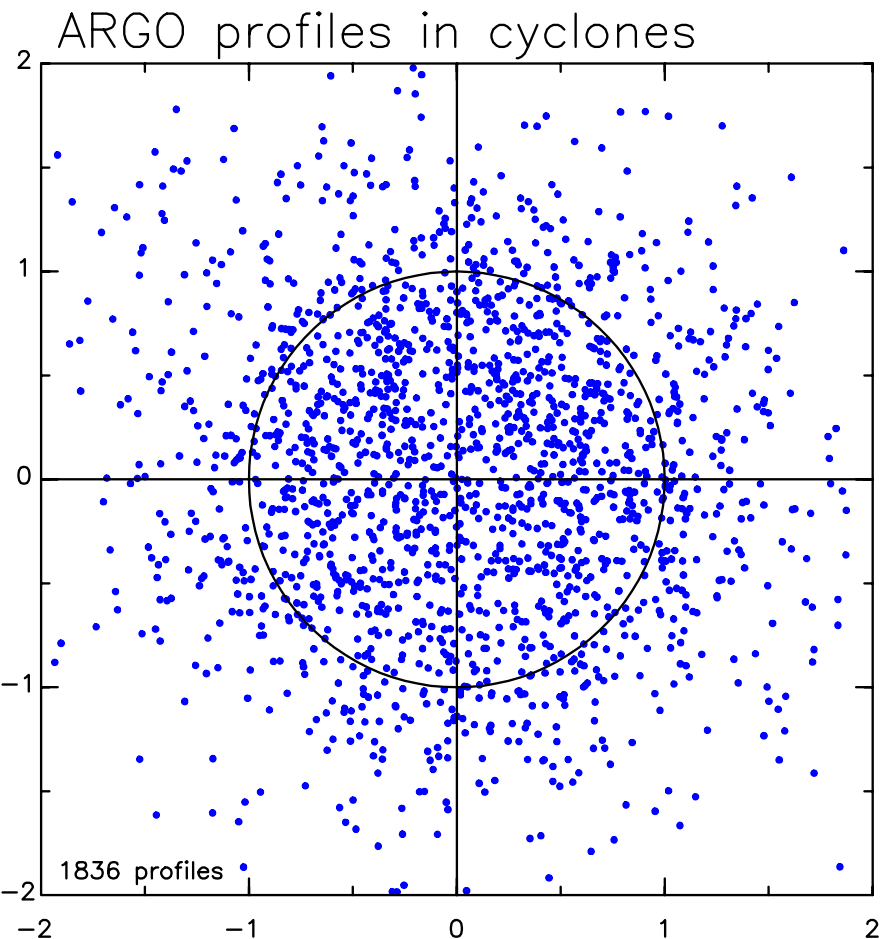
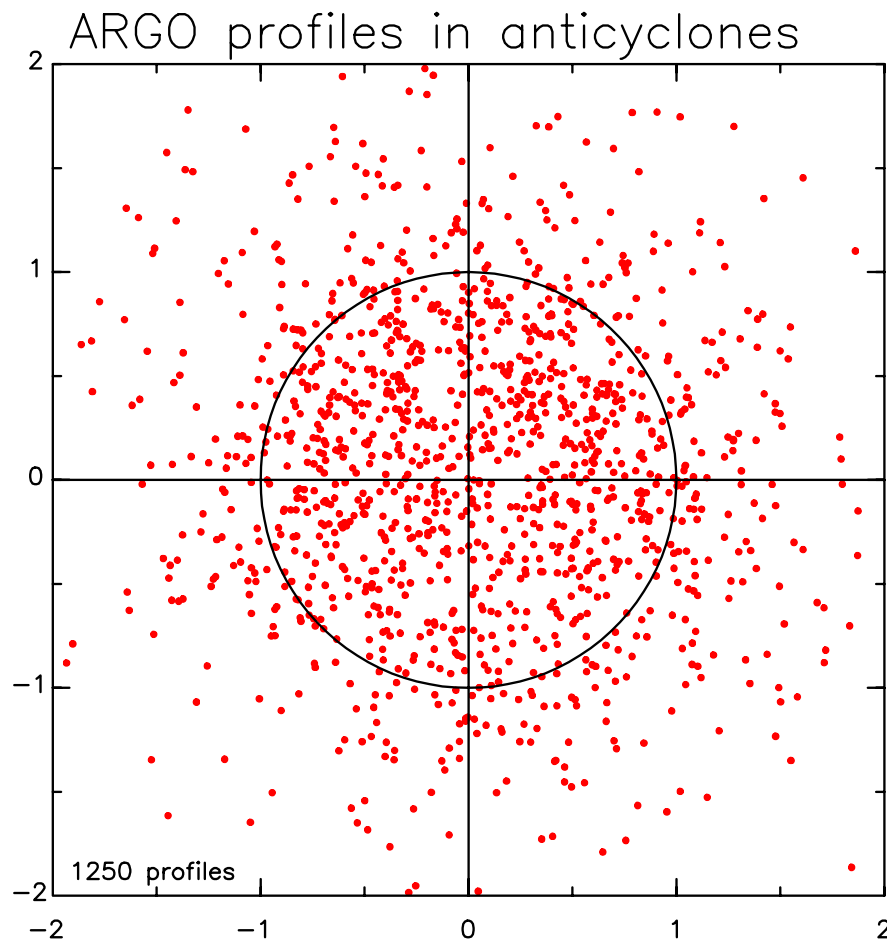


ARGO float profiles can be collocated with the locations of eddies.

Globally, 42% of all ARGO float profiles occurred within the interior of mesoscale eddies.

ARGO Float Profiles within Indian Ocean Eddies

ARGO profiles from which MLD seasonal cycle is calculated

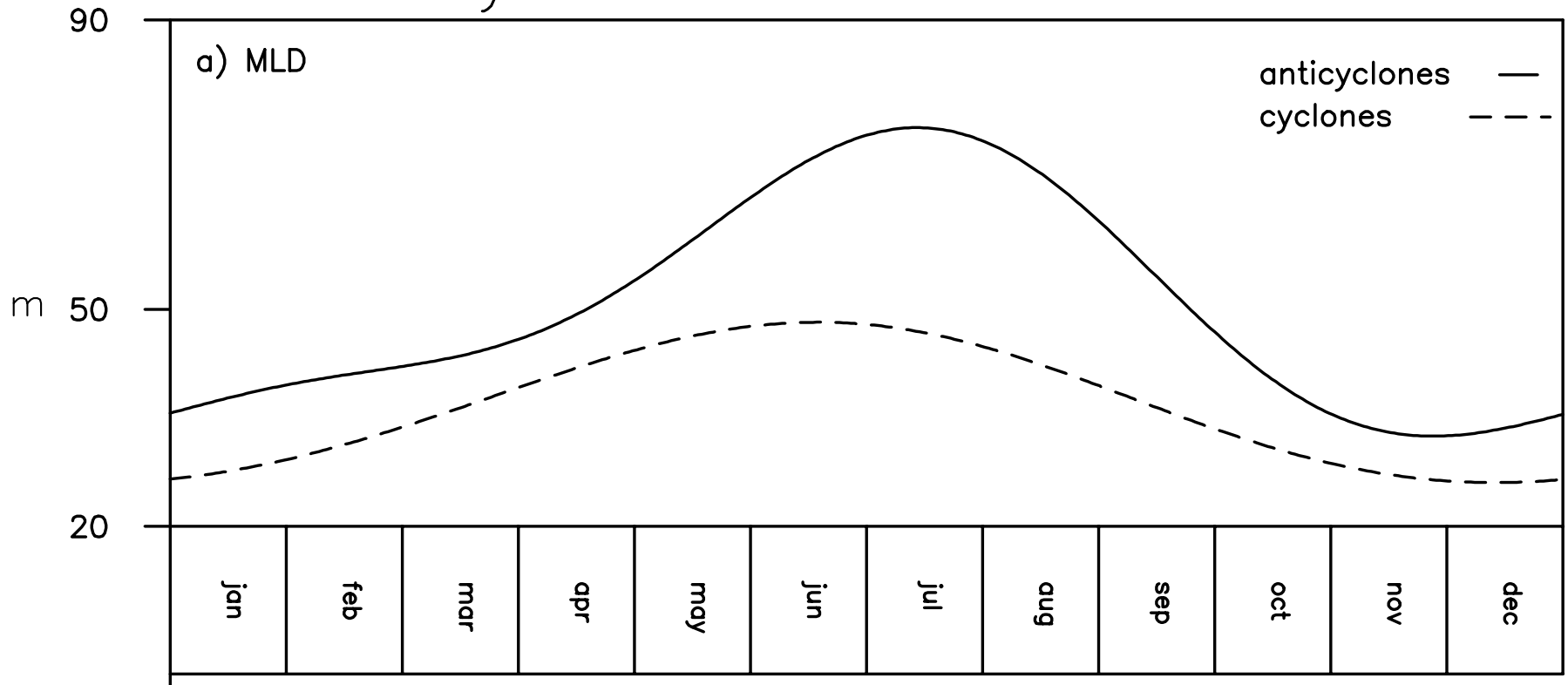


Seasonal cycles of MLD are calculated from the above profiles as a function of eddy polarity.

Seasonal Cycle of Mixed Layer Depth

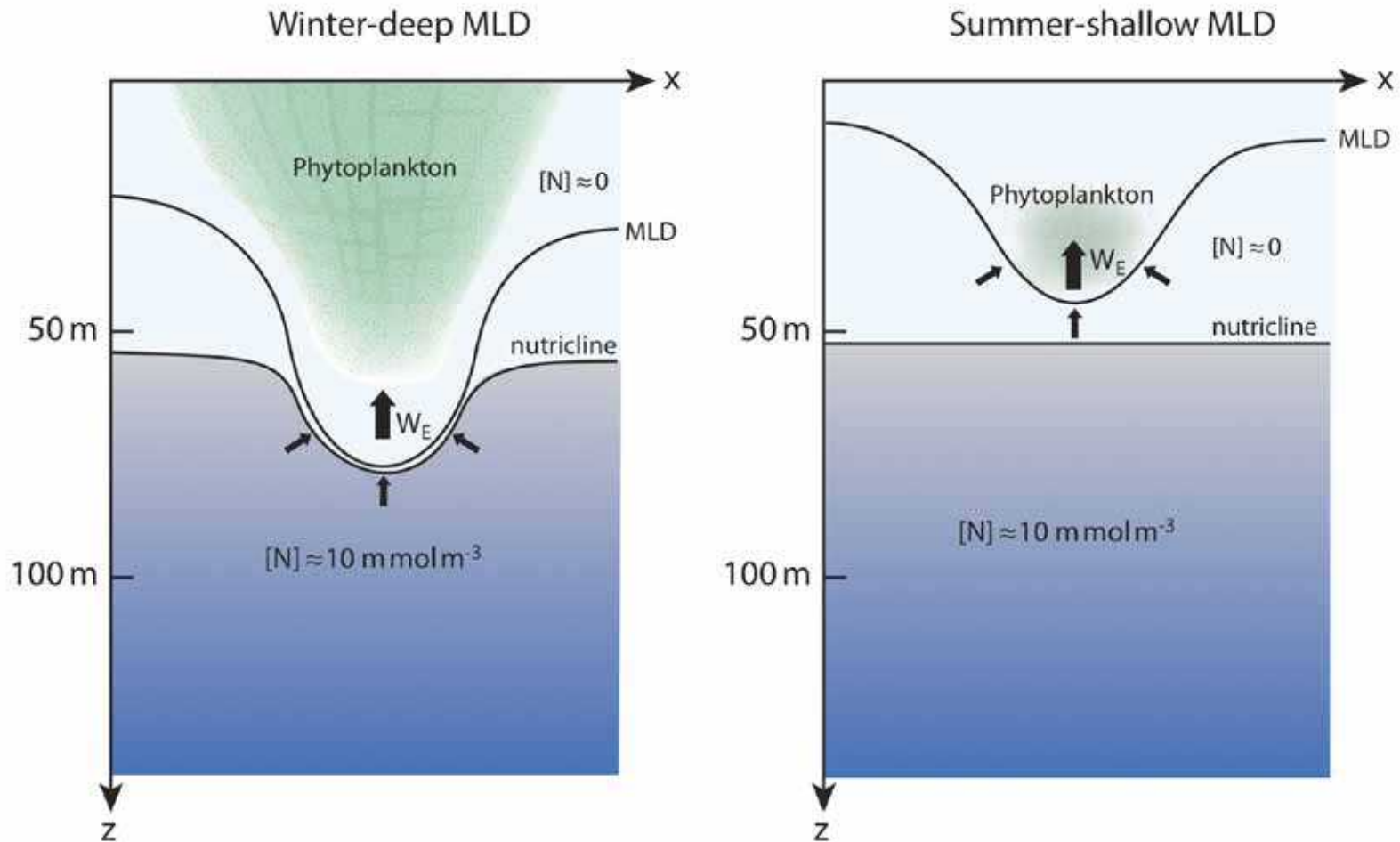
ARGO float profile MLD from density algorithm
(Holte and Talley, 2009, <http://mixedlayer.ucsd.edu/>)

seasonal cycle of MLD from ARGO



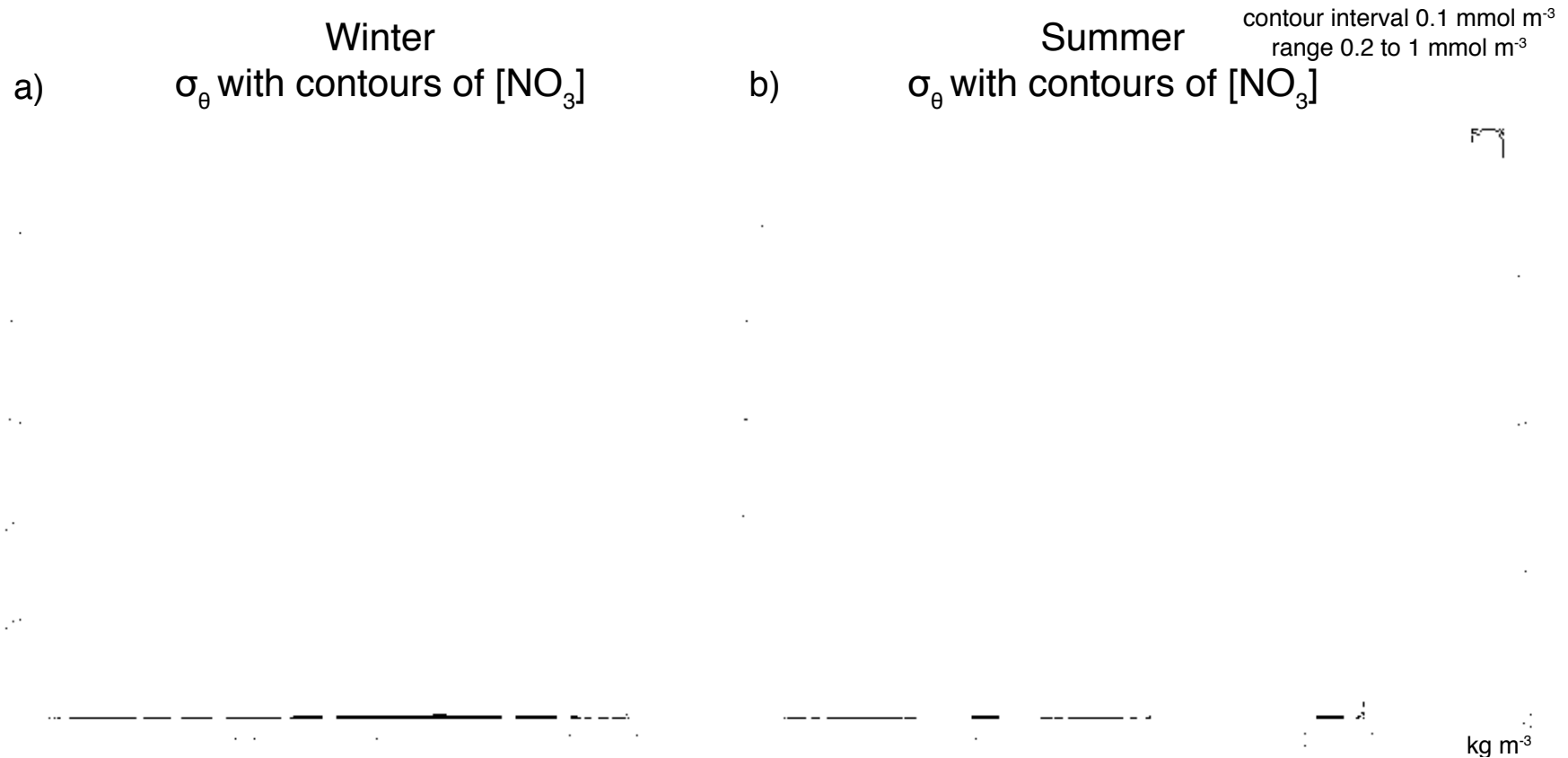
The biological response to eddy-induced Ekman pumping appears to be limited to times when the average MLD within anticyclones exceeds 50 m.

The Seasonal Decoupling of the Mixed Layer from the Nutricline



Can we see evidence of this decoupling in climatological nutrient and stratification data?

The Seasonal Decoupling of the Mixed Layer from the Nutricline



Seasonal and meridional averages of density overlaid with contours of nitrate concentration
(*World Ocean Atlas, 2005*)

Conclusion 2: Eddy-Induced Ekman Pumping

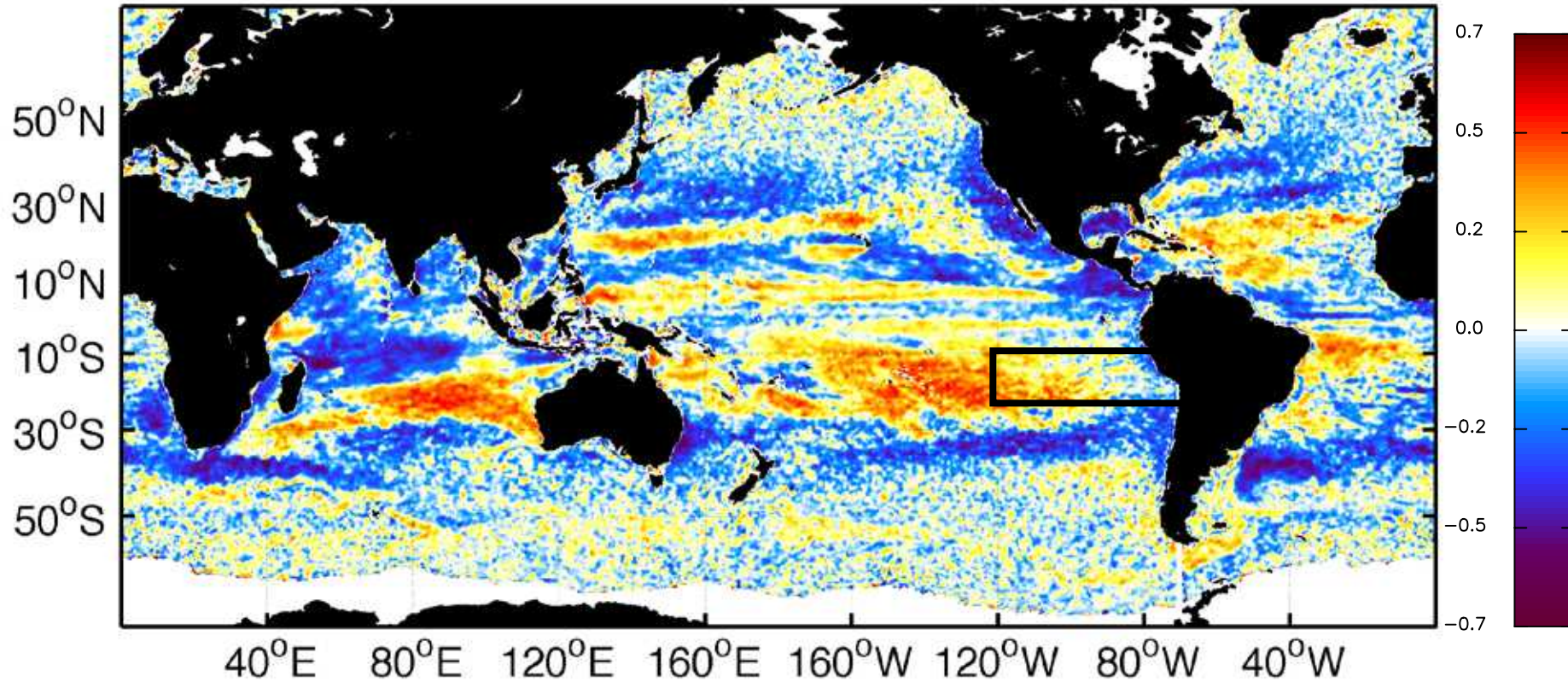
Eddies of the Southern Indian Ocean

1. A wide variety of other datasets were collocated to these eddies for this study:
 - Chlorophyll concentrations from SeaWiFS and MODIS-Aqua
 - Wind stress curl and hence Ekman pumping velocity from QuikSCAT
 - Mixed layer depth from ARGO floats
2. ARGO float observations provide valuable insight into the vertical structure of eddies tracked in merged altimetry observations.
3. Eddy-induced Ekman pumping appears to drive seasonal blooms in the cores of anticyclonic eddies in the Southern Indian Ocean.
4. The seasonal nature of these blooms appears to be linked to changes in mixed layer depth

Where do eddies influence marine ecosystems?

the influence of eddies on marine ecosystems is regionally dependent

SSH-CHL Cross Correlation



Regions of positive correlation are associated with CHL blooms in anticyclonic eddies

Regions of negative correlation are representative of cyclonic eddies driving increased CHL blooms

Westward Co-Propagation of SSH and CHL

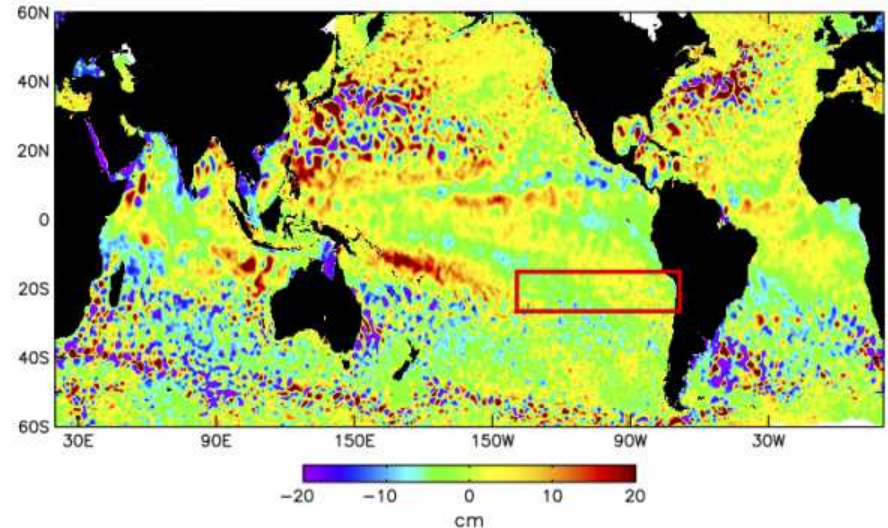
Numerous past studies have noted co-propagation of SSH and CHL anomalies:

- Cipollini et al. (2001, *Geophys. Res. Lett.*)
- Uz et al. (2001, *Nature*)
- Siegel (2001, *Nature*)
- Uz and Yoder (2004, *Deep-Sea Res.*)
- Dandonneau et al. (2003, *Science*)
- Killworth (2004, *Science*)
- Dandonneau et al. (2004, *Science*)
- Killworth et al. (2004, *J. Geophys. Res.*)
- Charria et al. (2003, *Geophys. Res. Lett.*)
- Charria et al. (2006, *J. Mar. Res.*)
- Charria et al. (2008, *Ocean Sci.*)
- Gutknecht et al. (2010,
- Chu and Kuo (2010, *Deep-Sea Res.*)
- and others.....

All of these studies have attributed the observed covariability to Rossby wave influence on CHL.

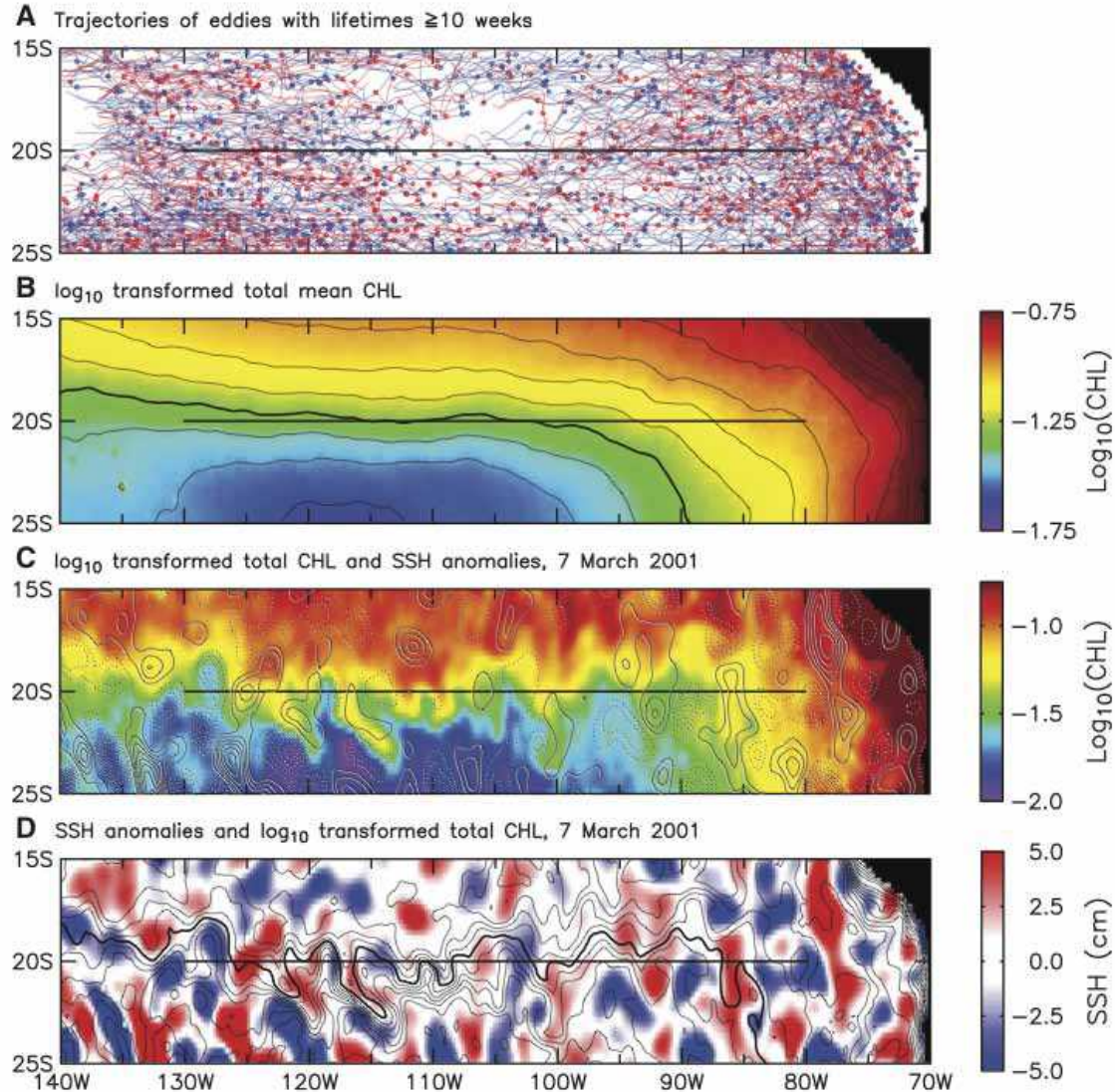
*The **southeastern subtropical Pacific** has been a region of particular focus and debate about the detailed mechanism by which Rossby waves influence CHL.*

The high-resolution merged altimeter dataset reveals that the physical influence on CHL is by nonlinear mesoscale eddies rather than Rossby waves.....



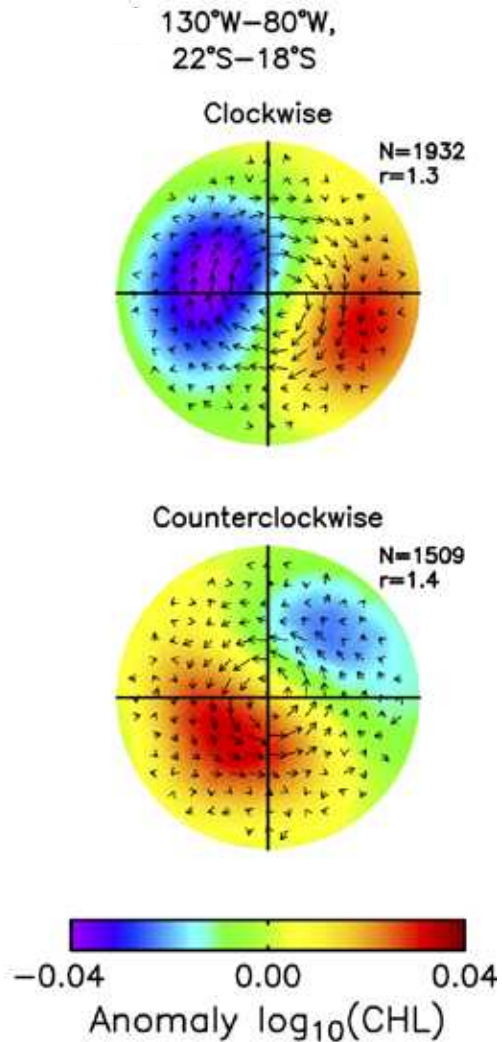
Eddies of the South Pacific

region investigated by Dandonneau et al., 2003; Killworth, 2004; Dandonneau et al., 2004 and Killworth et al., 2004



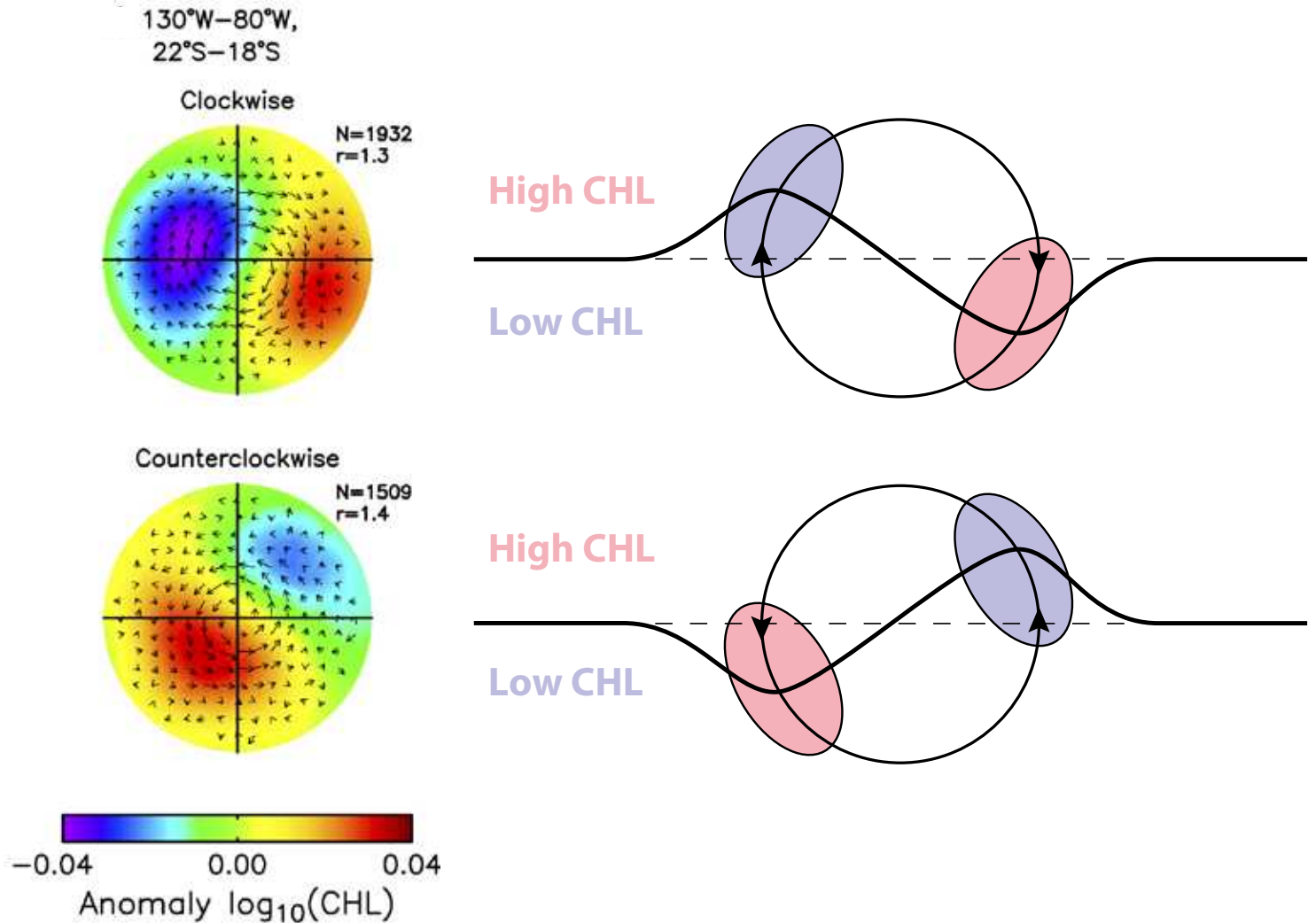
Eddy Composite Averages of Chlorophyll Anomaly

eddies along 20°S section



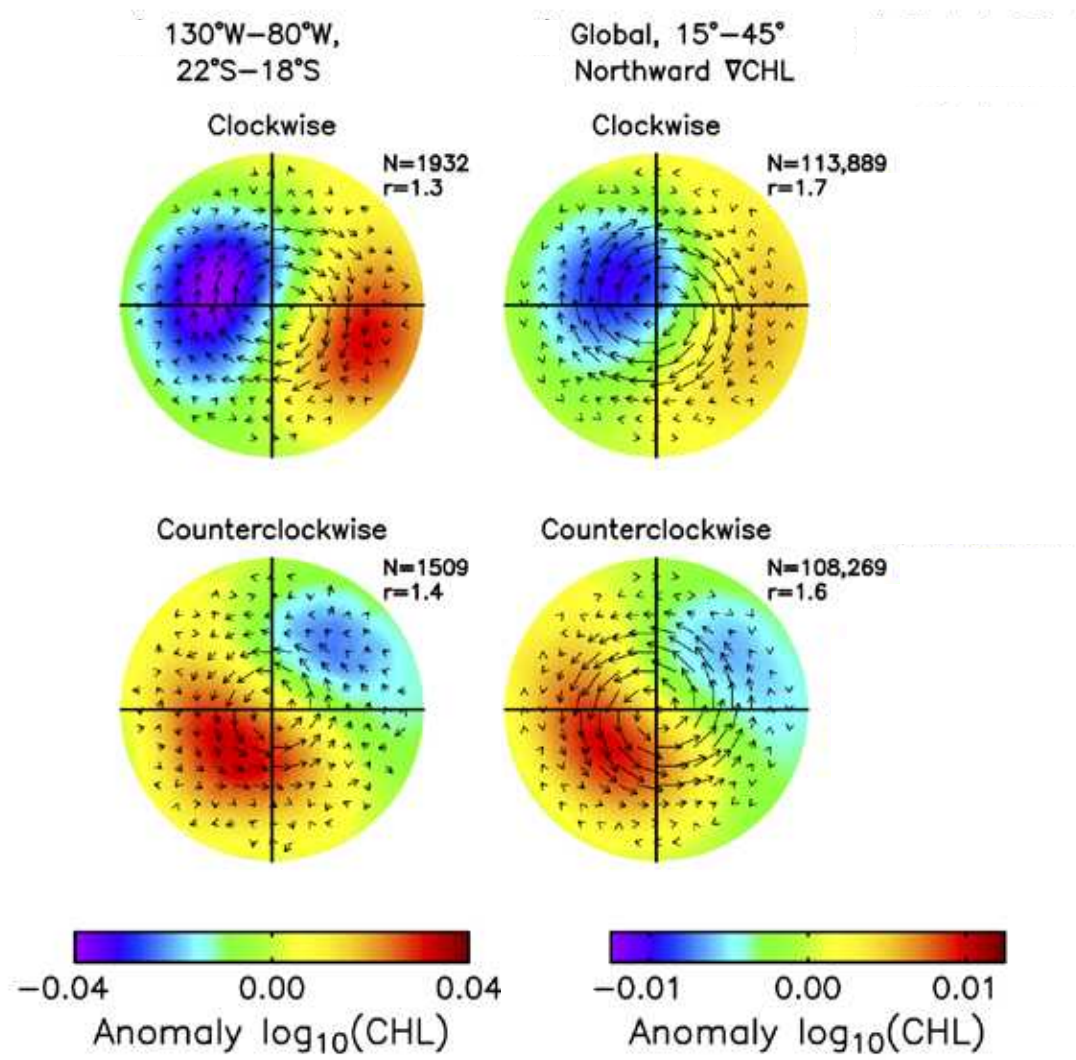
Eddy Composite Averages of Chlorophyll Anomaly

eddies along 20°S section



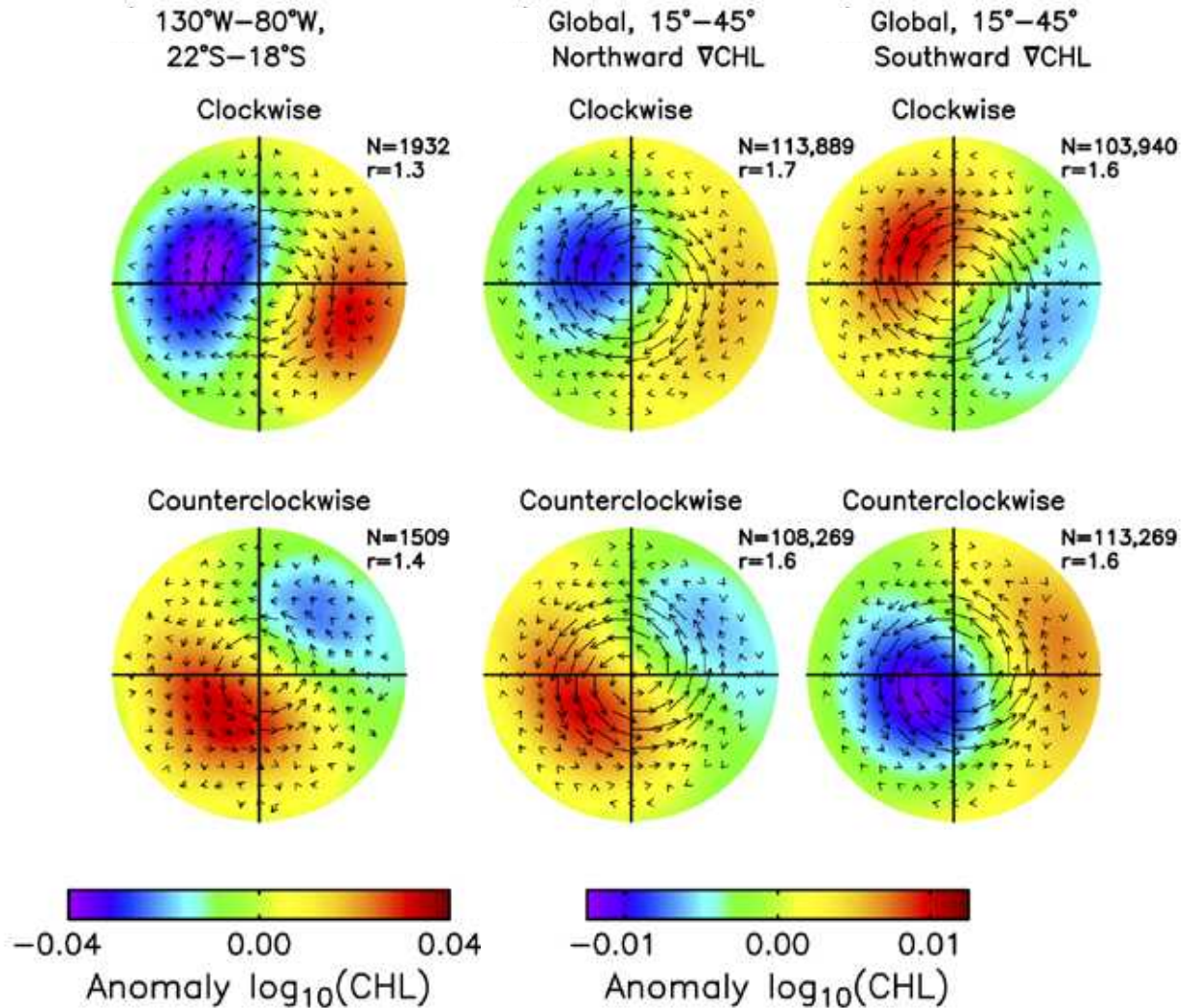
Global Composites of Chlorophyll Anomaly

northward CHL gradient



Global Composite of Chlorophyll Anomaly

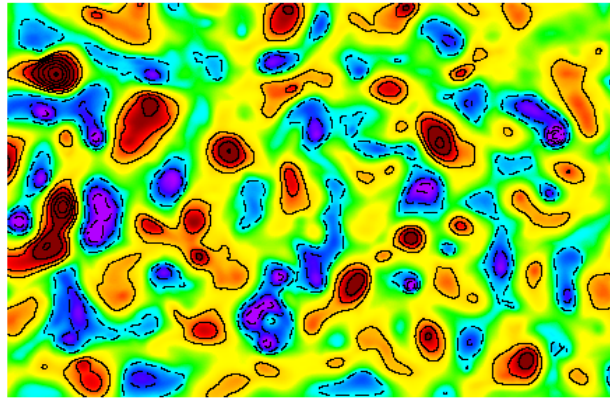
northward and southward CHL gradient



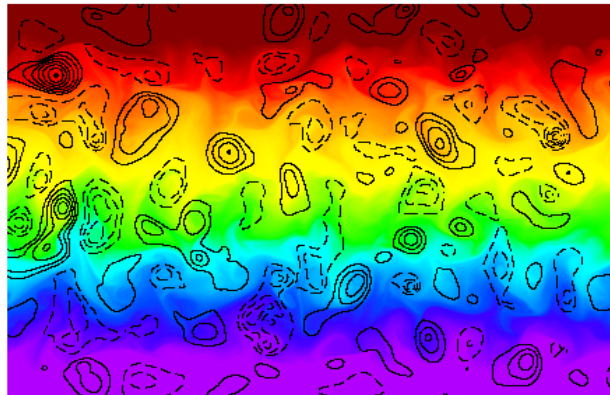
Reduced-gravity Quasigeostrophic Model

seeded with random Gaussian approximations of eddies around 20° in the Pacific

Sea Surface Height, Simulation Day 3000



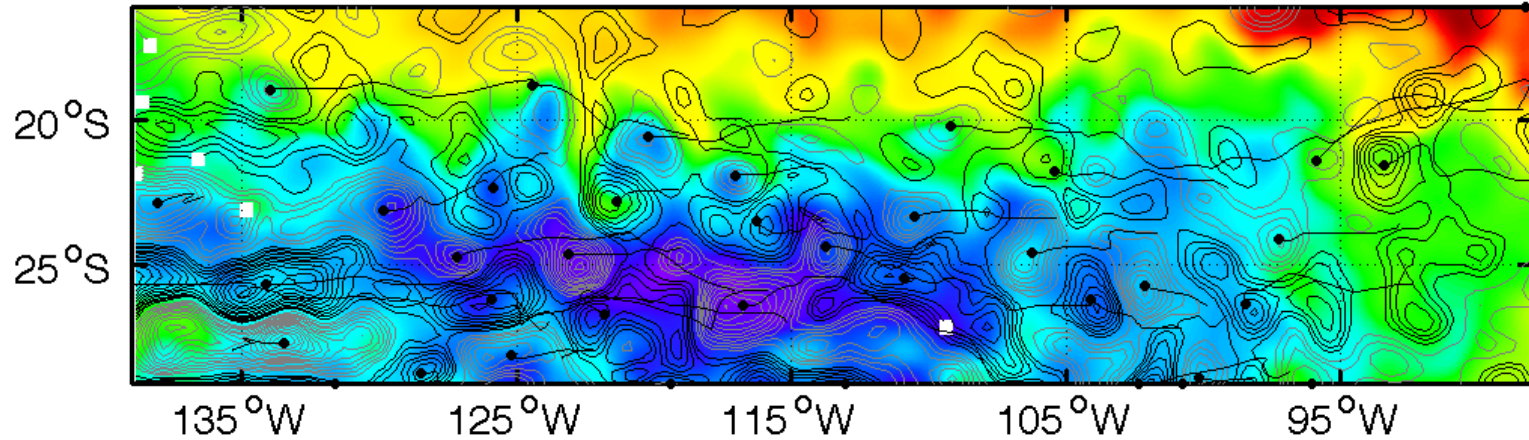
Tracer with 30-day Relaxation Time Scale



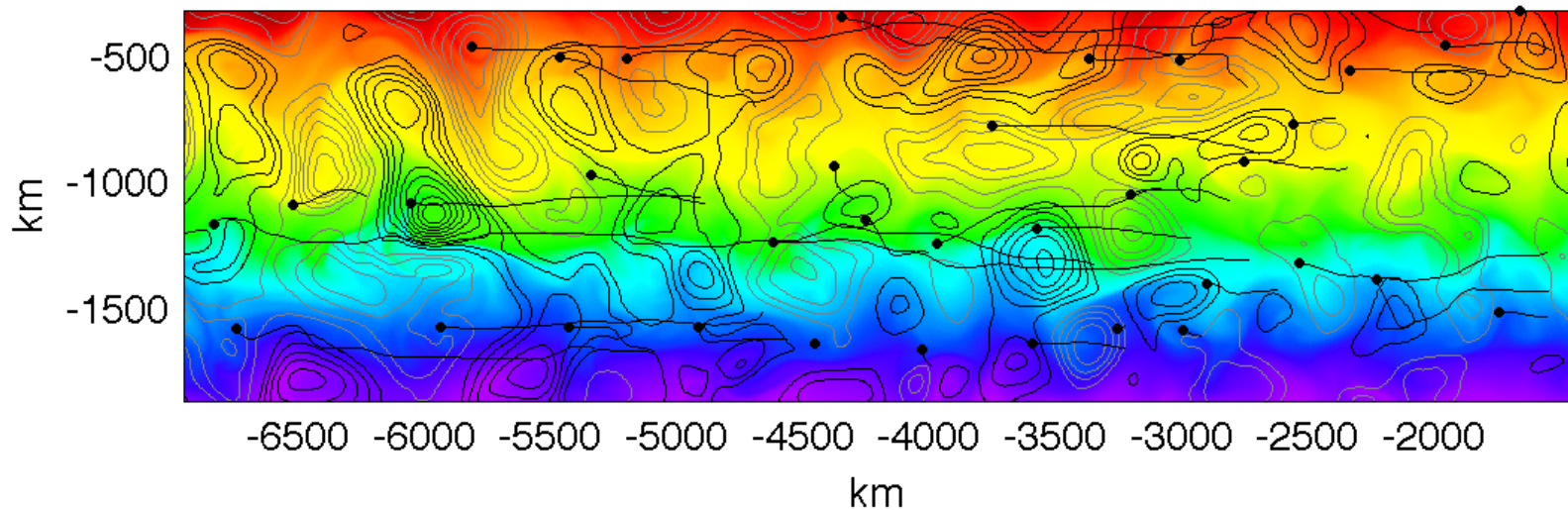
SeaWiFS Chlorophyll and QG Model

30-day average CHL smoothed $2^\circ \times 2^\circ$, QG model with 30-day relaxation time scale

Smoothed SeaWiFS Chlorophyll 2007-4-4

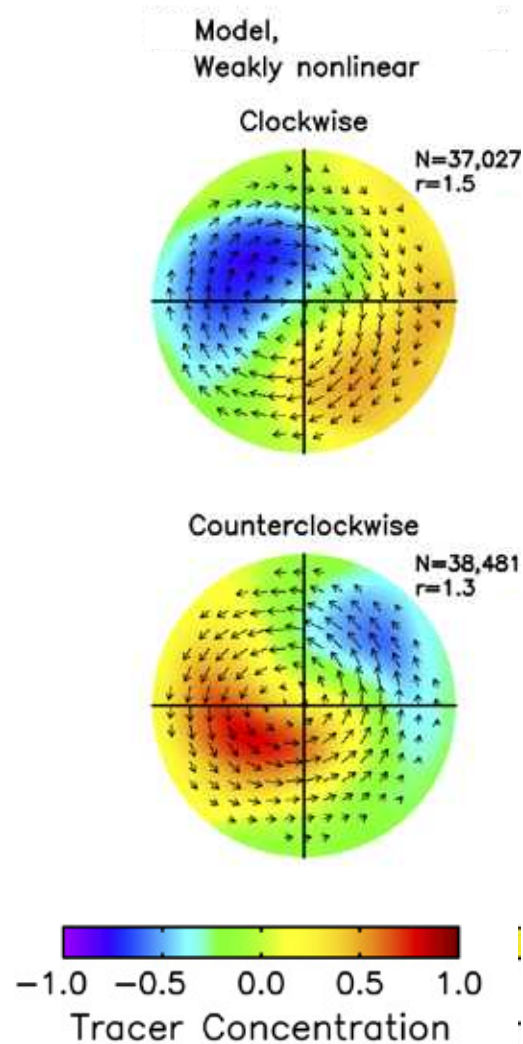


Quasigeostrophic Simulation Day



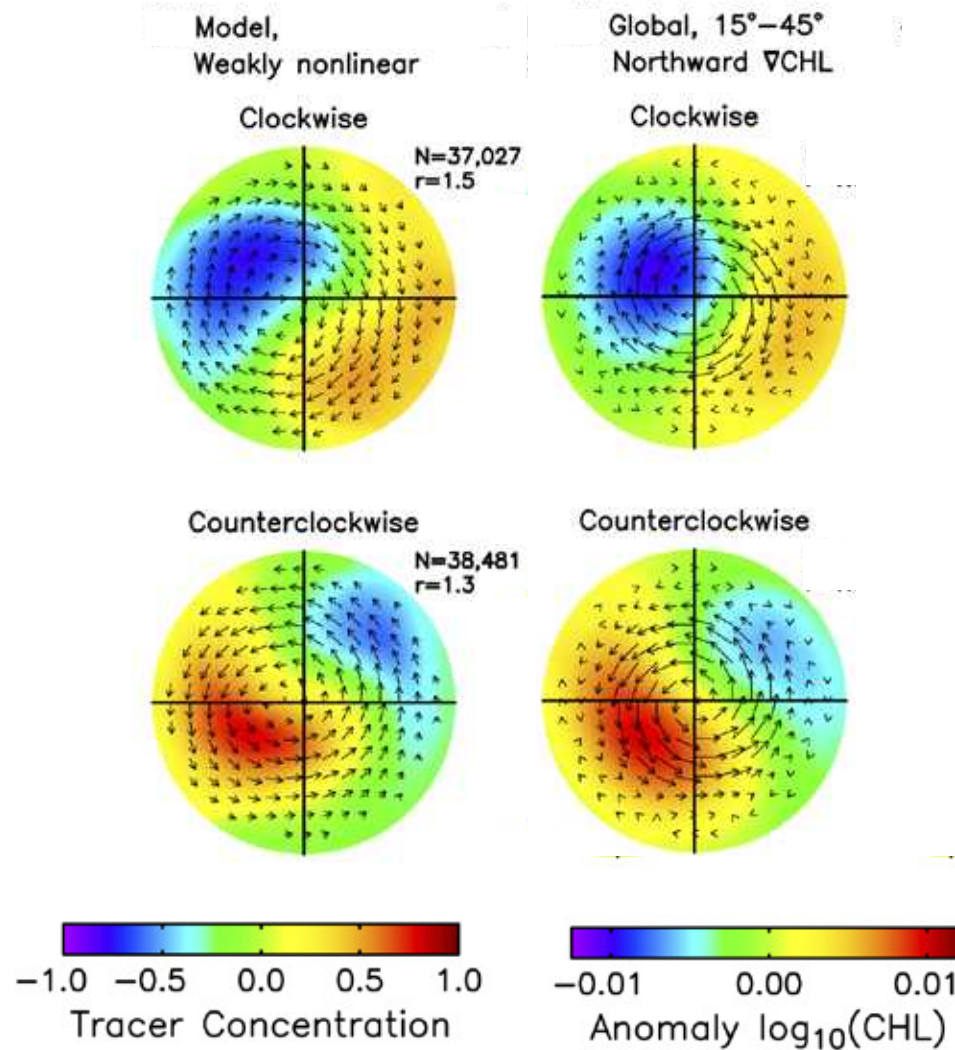
Composite Averages of Tracer in QG Model

model eddies in a meridionally varying tracer



Composite Averages of Tracer in QG Model

model eddies in a meridionally varying tracer



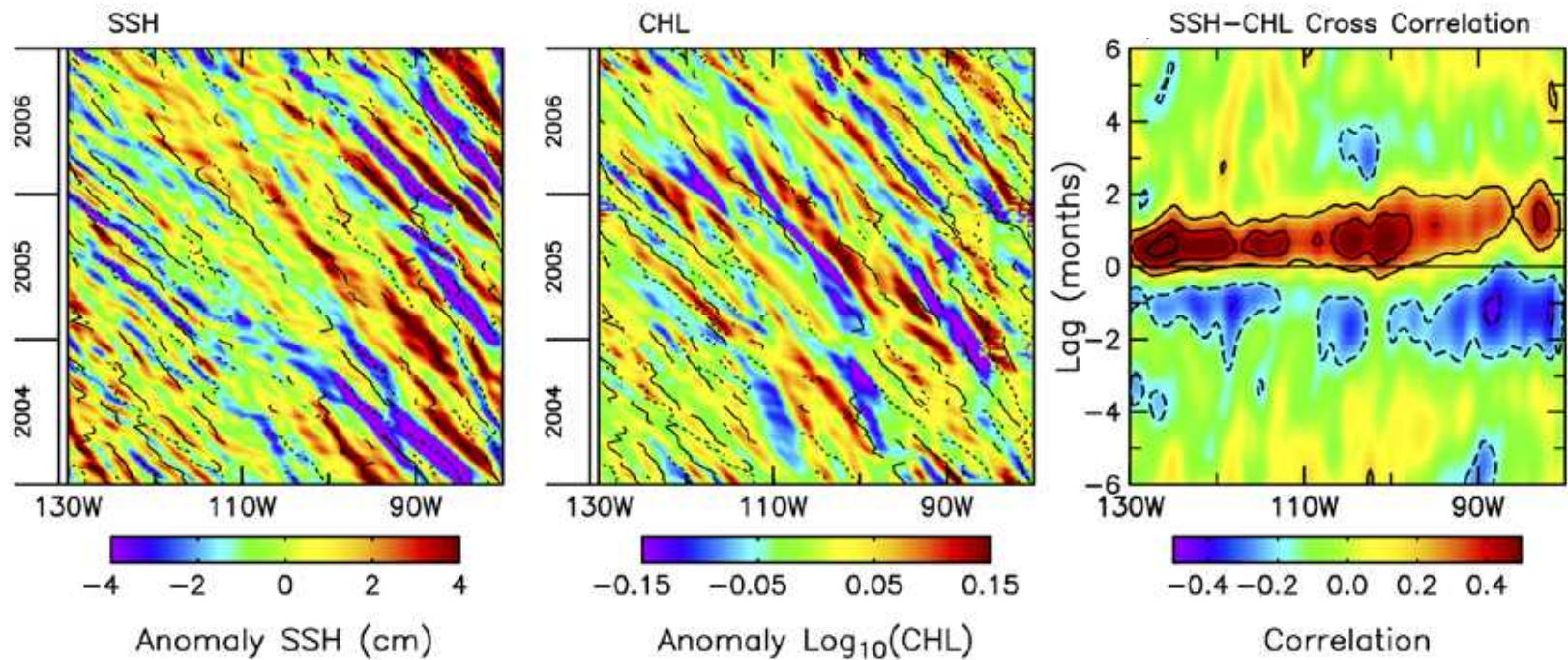
Conclusion 2: Advection of CHL around eddies

the “dominant” mechanism

- The collocation of CHL with the location and scale of eddies reveals that eddies act to advect CHL
- Statistically, the dominant mechanism by which eddies influence oceanic chlorophyll is stirring of the ambient chlorophyll field by azimuthal advection.
- Global eddy composite averages of chlorophyll are consistent with eddies in the Southeastern Pacific and QG model of passive tracer with finite relaxation time scale.
- Regionally, exceptions to this dominant mechanism can be observed (Southern Indian Ocean)

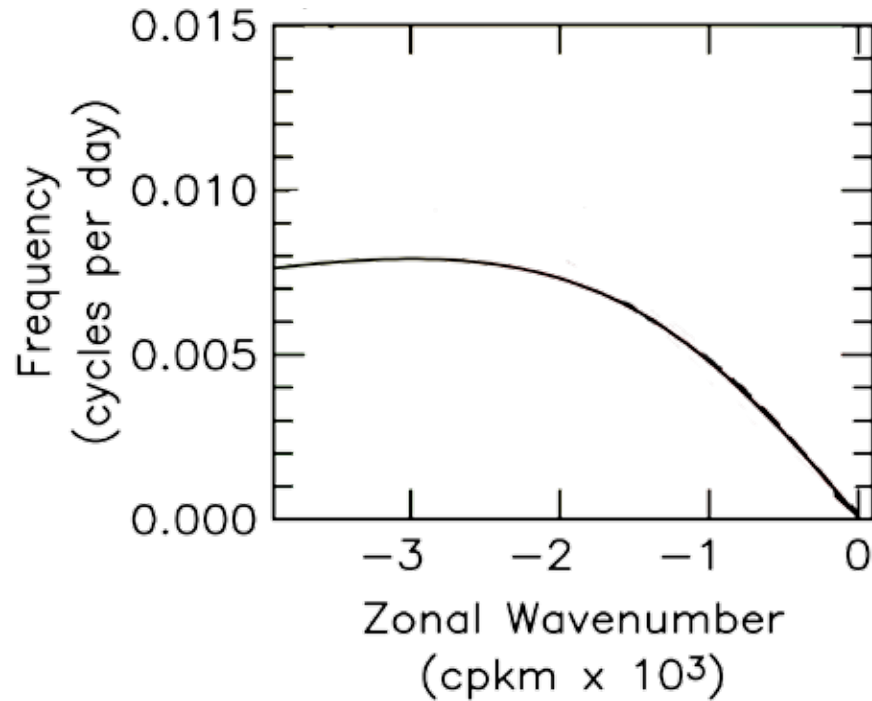
Westward Co-Propagation of Chlorophyll and SSH

zonal section of filtered CHL and SSH along 20°S



Westward Propagation of CHL and SSH

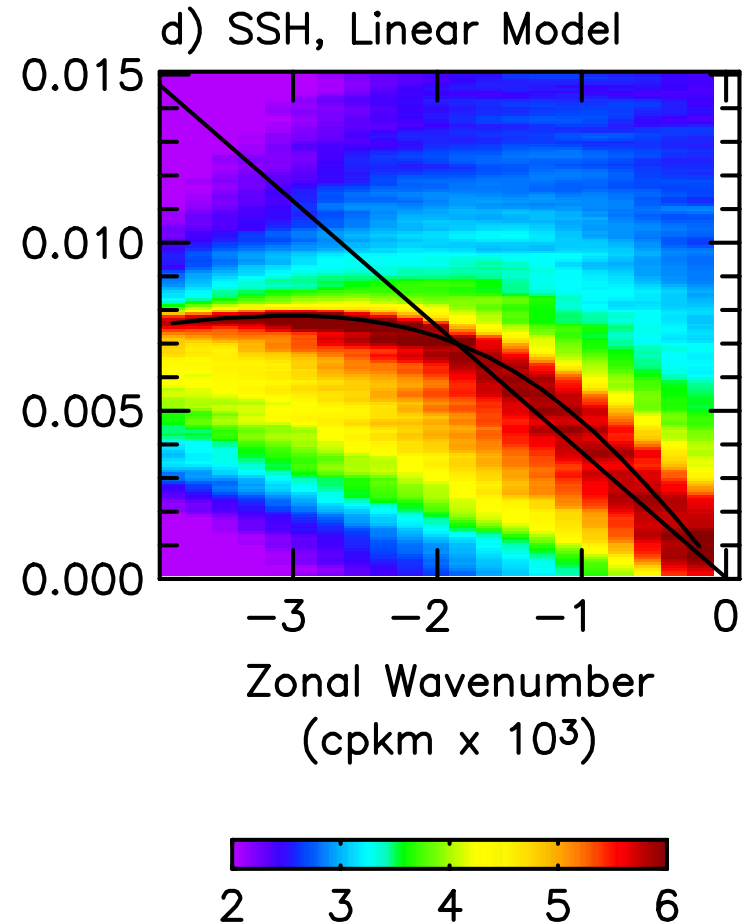
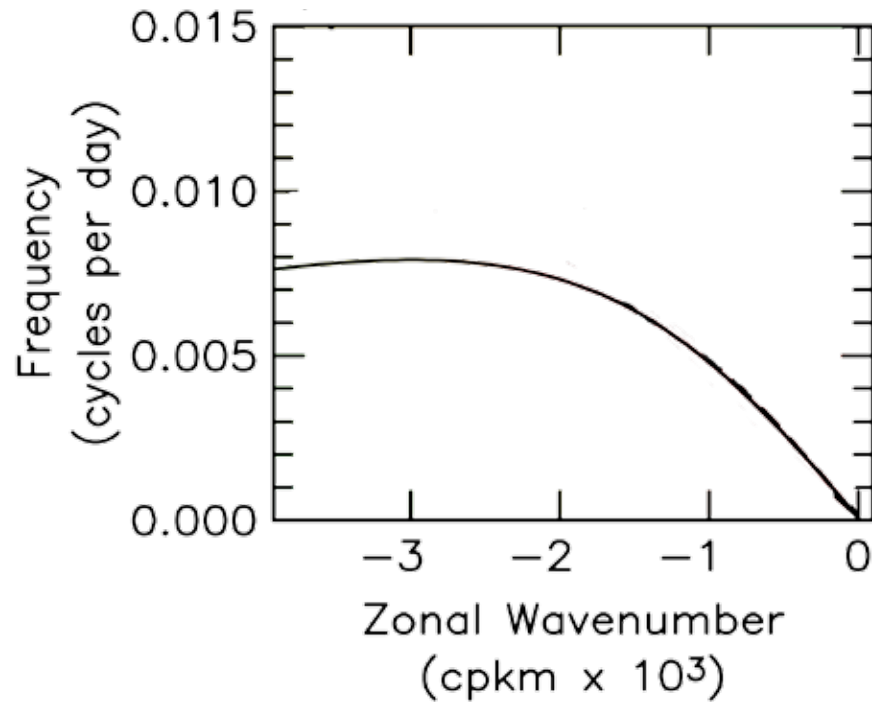
wavenumber-frequency power spectral density



$$\omega = \frac{-\beta k}{k^2 + \lambda_0^{-2}}$$

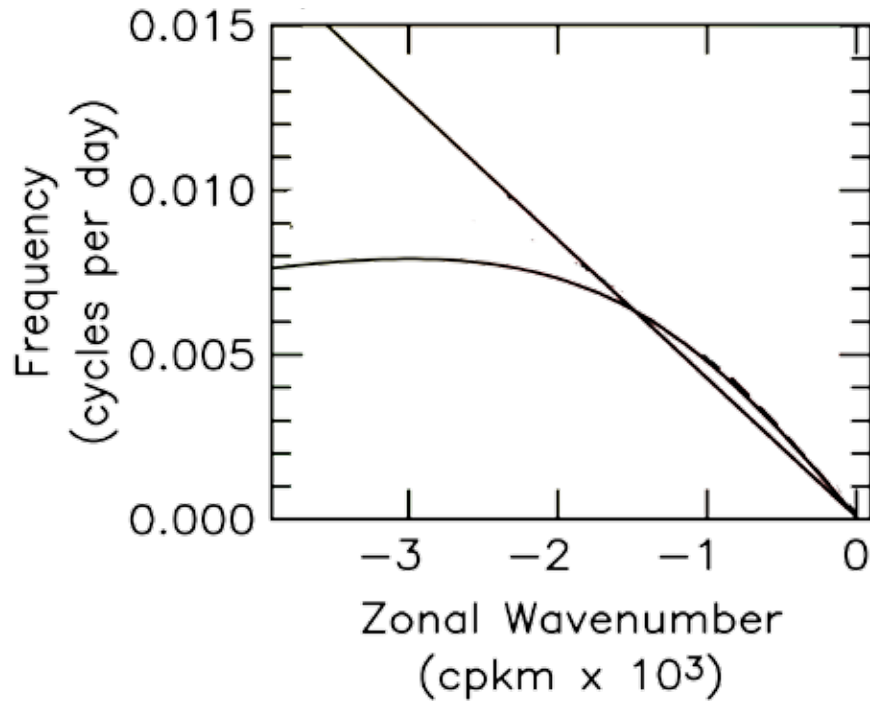
Westward Propagation of CHL and SSH

wavenumber-frequency power spectral density



Westward Propagation of CHL and SSH

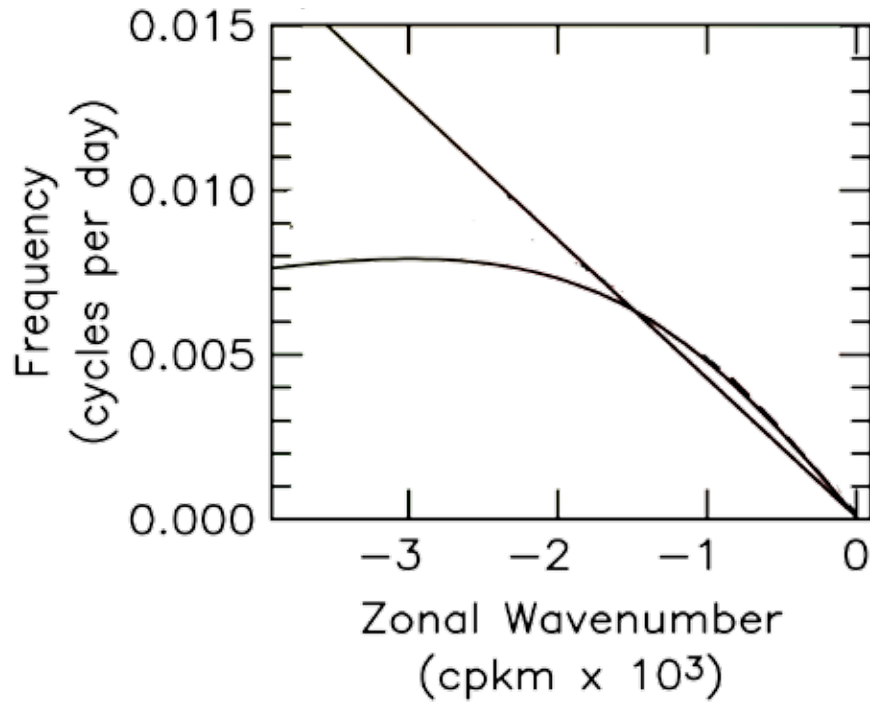
wavenumber-frequency power spectral density



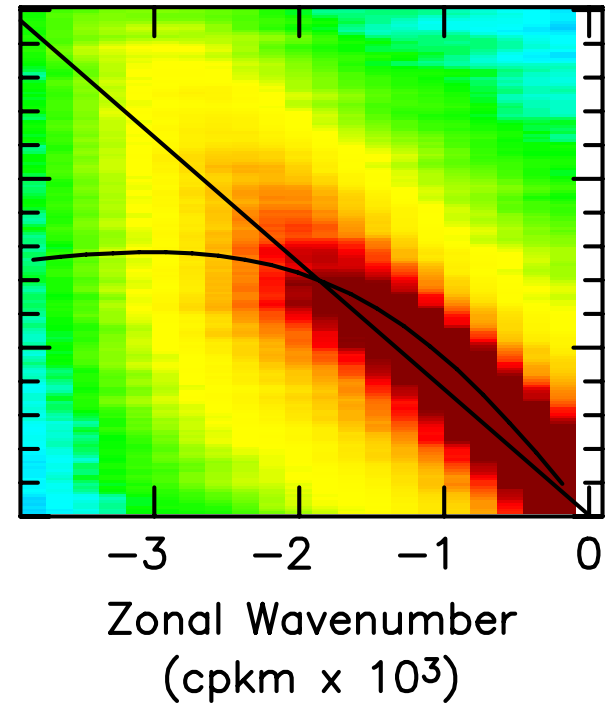
Avg. Zonal Propagation Rate of Eddies
 $= -4.9 \text{ cm s}^{-1}$

Westward Propagation of CHL and SSH

wavenumber-frequency power spectral density

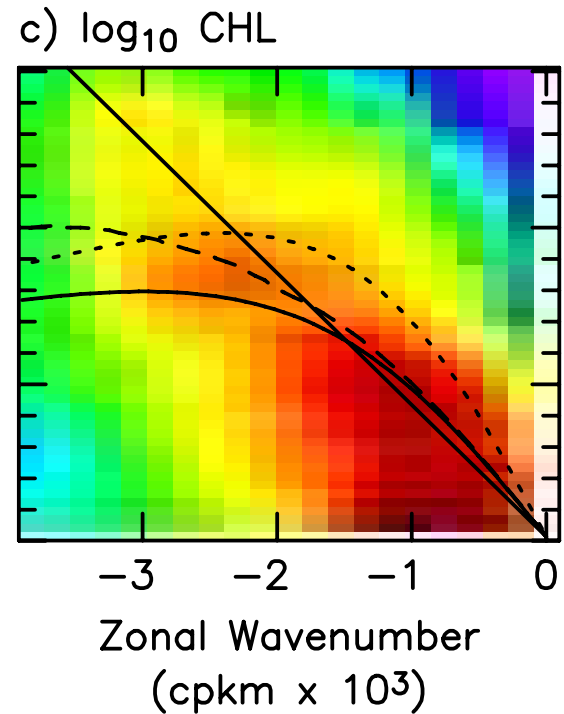
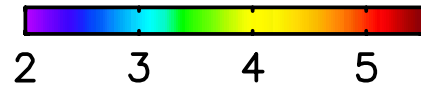
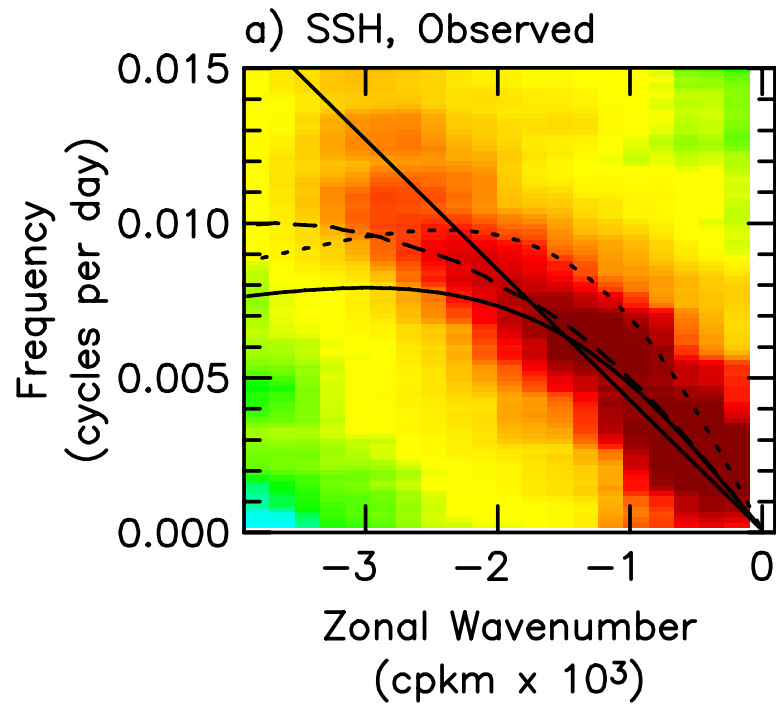


e) SSH, QG Model



Westward Propagation of CHL and SSH

wavenumber-frequency power spectral density



Conclusion 2: The Westward Propagation of SSH and Chlorophyll

mostly due to nonlinear eddies, not Rossby waves

- The observed westward co-propagation of CHL and SSH anomalies that in the past have been attributed to linear Rossby waves is in fact due to nonlinear eddies.
 - Phase relation (cross correlation) between SSH and CHL
 - Wavenumber-frequency spectra of CHL show that “most” of the energy in the westward propagating quadrant is at higher frequencies than allowed by linear Rossby waves.

The Influence of Nonlinear Mesoscale Eddies on Near-Surface Oceanic Chlorophyll

Dudley B. Chelton,^{1,2} Peter Gaube,¹ Michael G. Schlaz,¹ Jeffrey J. Early,² Roger M. Samelson³

Oceanic Rossby waves have been widely invoked as a mechanism for large-scale variability of chlorophyll (CHL) observed from satellites. High-resolution satellite altimeter measurements have recently revealed that sea-surface height (SSH) features previously interpreted as linear Rossby waves are nonlinear mesoscale coherent structures (referred to here as eddies). We analyze 10 years of measurements of these SSH fields and concurrent satellite measurements of upper-ocean CHL to show that these eddies exert a strong influence on the CHL field, thus requiring reassessment of the mechanism for the observed covariability of SSH and CHL. On time scales longer than 2 to 3 weeks, the dominant mechanism is shown to be eddy-induced horizontal advection of CHL by the rotational velocities of the eddies.

A decade of concurrent satellite measurements of sea surface height (SSH) and upper-ocean chlorophyll (CHL) is enabling studies of physical-biological interaction that are not feasible from ship-based observations. Although satellites provide only near-surface information about ocean physics and biology, they are the only practical means of obtaining dense, global observations. Altimetric measurements of SSH reveal that westward propagation is ubiquitous (1) with characteristics similar to the linear Rossby waves by which the ocean adjusts to wind and thermal forcing (2). Westward propagation is also evident in CHL estimates derived from satellite measurements of ocean color. The widespread interpretation of the westward-propagating SSH variations as Rossby waves led naturally to interpretations that the CHL variations are also induced by Rossby waves (3 – 5).

The mechanism for Rossby wave influence on CHL has been debated (4 – 9), in part because of inconsistency in the lag between variations of SSH and CHL. The most widely accepted view is that the covariability between SSH and CHL arises from cyclical advection of CHL by the horizontal velocity field associated with passing Rossby waves (7 – 9).

The prevailing view before the recent focus on Rossby wave influence was that CHL concentration is influenced by nonlinear eddies (10 – 15). Investigations of this eddy influence have continued in parallel with Rossby wave studies. Here, we show that the copropagation of CHL and SSH previously interpreted as having been

caused by Rossby waves is in fact attributable to eddies.

Nonlinearity of SSH variability. High-resolution SSH fields produced by merging the measurements from two simultaneously operating satellite altimeters (16) reveal that westward-propagating features previously believed to be linear Rossby waves are actually nonlinear rotating coherent structures (“eddies”) with radii of ~ 100 km (17 , 18). Because such mesoscale features propagate westward with approximately the speed of long Rossby waves (17 – 19), they can masquerade as Rossby waves in low-resolution SSH fields constructed from measurements by a single altimeter.

The degree of nonlinearity of a mesoscale feature is characterized by the ratio of the rotational fluid speed U to the translation speed c of the feature. When $U/c > 1$, the feature is nonlinear, which allows it to maintain a coherent structure as it propagates (20). This requires that all of the wavelength components of the feature propagate at the same speed, i.e., nondispersively. With linear Rossby wave dynamics, features that are initially spatially compact quickly lose their coherent structure through dispersion (21).

At latitudes higher than 25° , 98% of the features tracked for ≥ 10 weeks have $U/c > 1$ (fig. S2). The degree of nonlinearity is slightly less at lower latitudes where the propagation speeds c are faster (17 , 18). But even in the latitude range 15° to 25° , 95% of the tracked features have $U/c > 1$ (fig. S2).

Westward copropagation of SSH and CHL. The revised interpretation of westward-propagating SSH as nonlinear eddies mandates a reassessment of past conclusions that the westward copropagation of CHL and SSH is indicative of Rossby wave influence on CHL. The alternative hypothesis that CHL variability is eddy-induced is

examined here from 10 years of concurrent measurements of SSH and CHL in the southeastern Pacific (SEP) near 20°S that has been a focus of past studies (6 , 7).

The trajectories of mesoscale eddies (18) in the SEP are shown in Fig. 1A. Compared with eddies observed globally in the latitude range 15° to 25° , their mean amplitude is smaller (3.2 cm versus 6.2 cm) but their mean radius is the same (110 km). Because U is approximately proportional to eddy amplitude, eddies in the SEP are less nonlinear (fig. S2); 87% have $U/c > 1$.

The mean CHL distribution has a generally northward gradient over most of the SEP (Fig. 1B). The influence of eddies is evident from the sinusoidal character of the CHL field at any particular time (Fig. 1, C and D). The distortions of an otherwise smoothly varying CHL field are most apparent in regions of strong CHL gradient.

Eddy influence on the CHL field becomes clearer after filtering to remove the large-scale and seasonally varying CHL and SSH (22). Westward copropagation of CHL and SSH is apparent from time-longitude plots of the resulting anomaly fields (Fig. 2, A and B). The trajectories of the centroids of clockwise (CW) and counterclockwise (CCW) rotating eddies in the SEP coincide, respectively, with negative and positive extrema of westward-propagating SSH (Fig. 2A). The positive lag of maximum positive correlation in Fig. 2C indicates that the SSH extrema at the eddy centroids lag the extrema of westward-propagating CHL by ~ 1 month in the eastern SEP, decreasing to ~ 0.5 month in the west. There is a weaker negative correlation at negative lags of 1 to 1.5 months.

Eddy influence on CHL. To interpret the lagged correlations in Fig. 2C, anomaly CHL was composite averaged within eddy interiors in a translating and rotated coordinate system in which the large-scale CHL gradient vector is oriented at a polar angle of 90° (22). The CHL anomaly composites consist of dipoles with opposing signs and with different orientations in CW and CCW rotating eddies (Fig. 3A). As indicated by the ratio r in Fig. 3A, the dipoles are asymmetric in both cases with larger magnitudes in the left half of each composite, corresponding to the leading half of these westward-propagating eddies. The displacements from the eddy centroid are smaller for these primary poles than for the secondary poles of opposite sign in the trailing (right) halves of the eddies (see also fig. S4).

The negative extremum of SSH at the centroids of CW rotating eddies in the SEP is straddled by negative and positive poles of CHL to the west and east, respectively. The opposite occurs in CCW rotating eddies, for which the positive extremum of SSH at the centroids is straddled by positive and negative poles of CHL to the west and east, respectively. The parallel bands of positive and negative lagged correlations in Fig. 2C thus arise from a combination of west-

¹College of Oceanic and Atmospheric Sciences, 104 COMS AB Innovation Building, Oregon State University, Corvallis, OR 97331-2533, USA. ²Northwest Research Associates, Post Office Box 3027, Bellevue, WA 98009, USA.

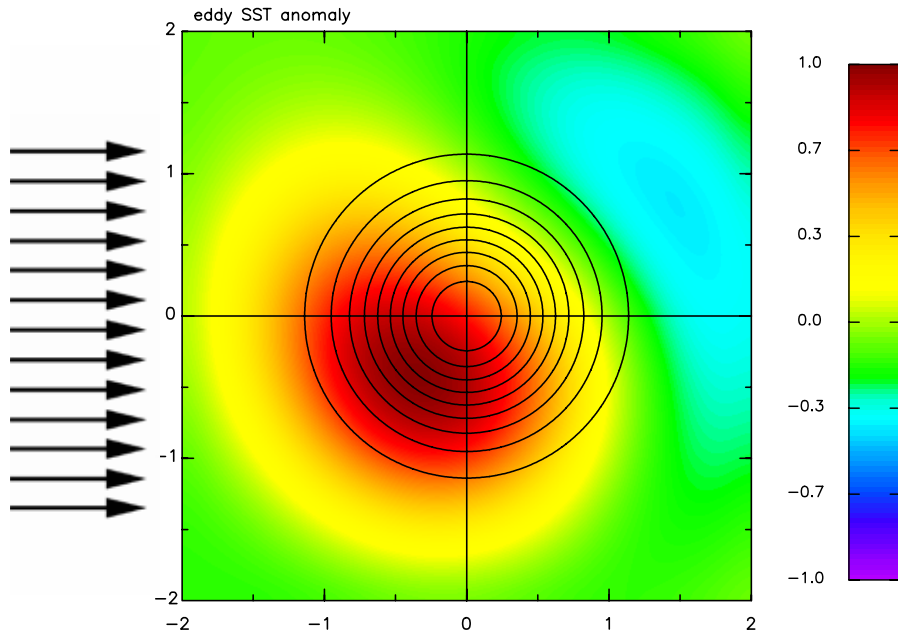
³To whom correspondence should be addressed. E-mail: rchelton@coas.oregonstate.edu

SST-Induced Ekman Pumping

How it works:

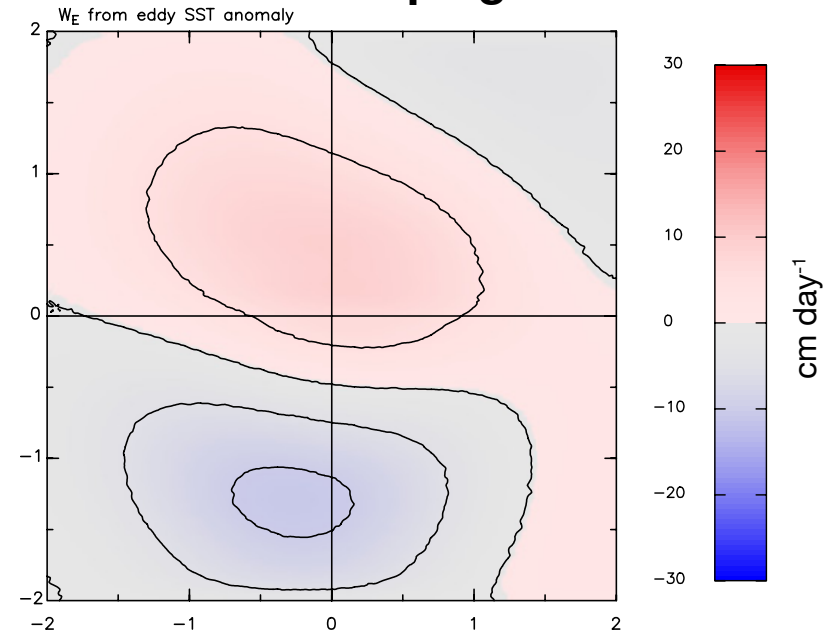
- Warm (cold) SST anomalies accelerate (decelerate) local winds resulting in a wind stress curl from the crosswind SST gradient associated with the SST anomaly.

SST'



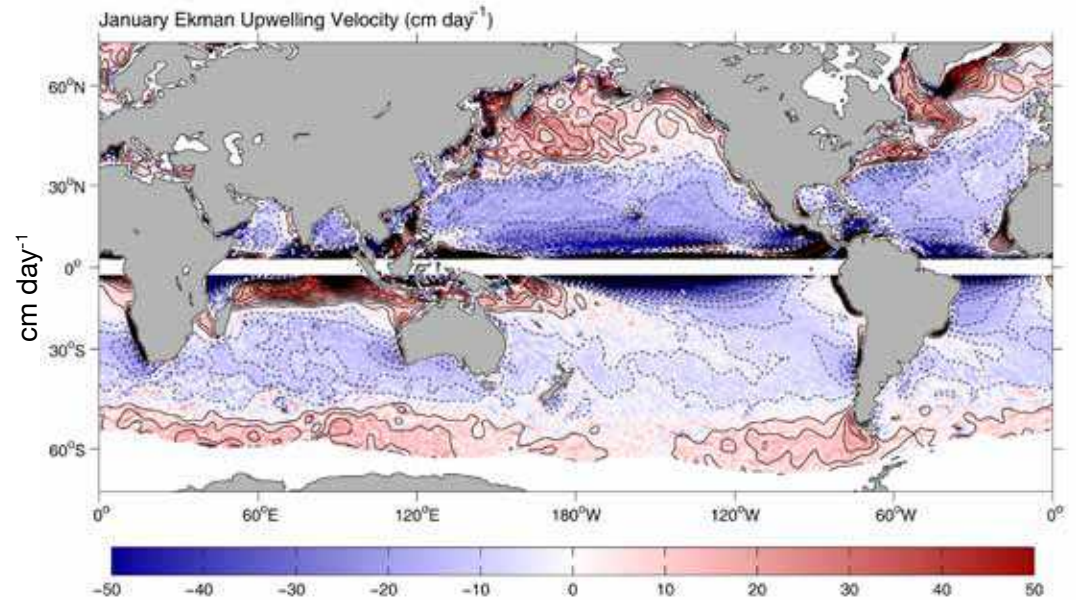
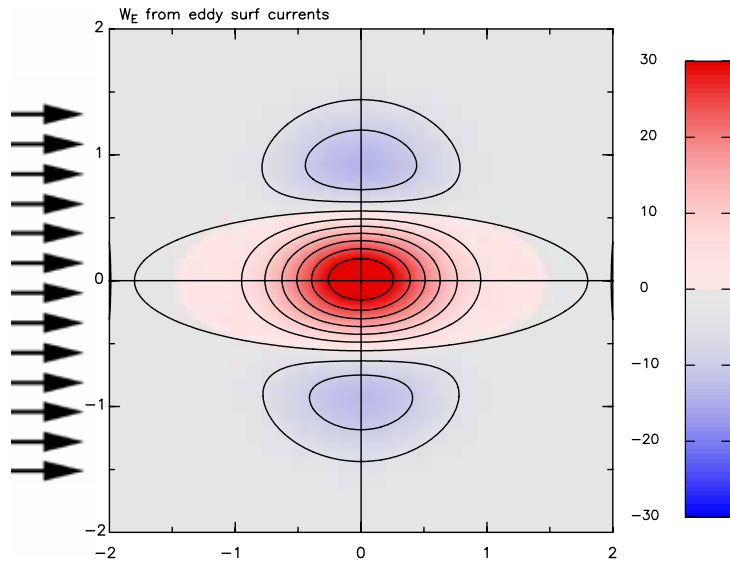
- 30°S
- 20 cm amp.
- 10 ms⁻¹ wind
- 1° SST pert.

SST-Induced Ekman Pumping



$$U'_{wind} = \alpha SST'$$
$$\alpha = 0.32$$

Eddy-Induced Ekman Pumping



Risien and Chelton, 2008

- *Eddy-induced Ekman pumping is of the same order of magnitude as basin scale Ekman pumping*